THESIS

# GEOMORPHIC EFFECTS OF INCREASED WOOD LOADING ON HYPORHEIC EXCHANGE FLOW

Submitted by

Ethan Ader

Department of Geosciences

In partial fulfillment of the requirements

For the Degree of Master of Science

Colorado State University

Fort Collins, Colorado

Summer 2019

Master's Committee:

Advisor: Ellen Wohl

Sara Rathburn
Ryan Morrison

ABSTRACT

GEOMORPHIC EFFECTS OF INCREASED WOOD LOADING ON HYPORHEIC EXCHANGE FLOW

Much of the recent scientific literature in the field of fluvial geomorphology has documented the benefits of the presence of large wood in rivers. One of these benefits is enhanced hyporheic exchange flow (HEF). Enhanced HEF has numerous benefits and therefore plays an important role in stream health. While the science of hyporheic exchange has progressed over the past few decades, studies thus far have focused on single pieces of wood or single jams. There have not yet been studies that examine whether multiple consecutive jams have an additive or nonlinear effect on HEF. This study focuses on the impacts of increased wood loading on geomorphic complexity and HEF. We examined relations among wood load, geomorphic complexity, and HEF by studying four different reaches along Little Beaver Creek, a 3rd order tributary to the Cache la Poudre River in the Colorado Front Range within the Arapaho and Roosevelt National Forest: 1) a single channel with no logjams, 2) a single channel with limited logjams, 3) an anabranching channel with limited logjams, and 4) an anabranching channel with abundant logjams. Pearson correlations were used to analyze the relationship between HEF, wood loading, and geomorphic complexity. We found that increased wood loading increases the volume of both pools and accumulated fine sediment at the reach level. Additionally, HEF positively correlates with geomorphic complexity and wood loading. The metrics that most strongly correlated with enhanced HEF all represent factors expected to increase connectivity from the channel to the hyporheic zone. These preliminary results suggest

that it is through this mechanism of increasing hyporheic zone connectivity that HEF is enhanced.

TABLE OF CONTENTS

LIST OF TABLES

LIST OF FIGURES

## 1 - Introduction

Large wood (>1 m long and >10 cm diameter; LW) is being implemented in river restoration projects at an increasing rate. This increase in usage is linked to the numerous benefits associated with the presence of LW (Wohl, 2017). One of these benefits is enhanced hyporheic exchange flow (HEF). HEF is the exchange of water between the channel and the shallow subsurface. This exchange occurs vertically into the bed of the channel and laterally into the banks. The shallow subsurface beneath a river corridor is known as the hyporheic zone, which can be defined as the region characterized by having flow paths that originate and terminate in the channel (Boulton et al. 1998; Tonina and Buffington, 2009). Enhanced HEF has numerous benefits and therefore plays an important role in stream health.

LW, which includes both individual pieces and jams, enhances HEF due to the ways in which LW physically alters both flow within channels and the channels themselves. The LW load ($m^3/m$) affects the magnitude of these physical impacts. Furthermore, channels are altered more by jams than by individual pieces of LW (Wohl, 2017). A jam is defined as a grouping of three or more pieces of LW that touch. Additionally, channel-spanning features likely alter channels more than features that only partially span the channel (Keller and Swanson, 1979). Table 1 summarizes ways in which LW can physically alter channels.

**Table 1 – Summary of the impacts of LW**

| Potential impact of LW | Citations |
|---|---|
| Increases flow resistance | Manga and Kirchner, 2000; Curran and Wohl, 2003; Daniels and Rhoads, 2003 |
| Deflects flow towards the bed/banks | Beschta, 1983; Cherry and Beschta, 1989 |
| Increases local scour | Beschta, 1983; Cherry and Beschta, 1989 |
| Increases local stage by increasing local roughness | Beschta, 1983; Bocchiola, 2011 |
| Enhances deposition and accumulation of fine materials | Keller and Swanson, 1979; Beschta, 1983; Montgomery and Buffington, 1997 |
| Alters cross sectional geometry | Keller and Swanson, 1979; Wallerstein and Thorne, 2004; Gendaszek et al., 2012 |
| Alters bedforms and is associated with increased undulations of the bed elevation | Montgomery and Buffington, 1997; Curran and Wohl, 2003; Faustini and Jones, 2003; MacFarlane and Wohl, 2003 |
| Creates pools and associated backwater effects, slowing velocities, increasing depth immediately upstream, and creating turbulence | Beschta, 1983; Nakamura and Swanson, 1993; Abbe and Montgomery, 2003; MacFarlane and Wohl, 2003; Gendaszek et al., 2012; Davidson and Eaton, 2013 |
| Increases spatial heterogeneity of sediment in the bed | Buffington and Montgomery, 1999; Faustini and Jones, 2003; MacFarlane and Wohl, 2003 |
| Decreases grain size | Faustini and Jones, 2003 |
| Facilitates channel avulsions and shifts channels towards a multithread planform | Keller and Swanson, 1979; Abbe and Mongomery, 2003; O'Connor et al., 2003; Collins et al., 2012; Wohl, 2011b |
| Stabilizes multithread channels | Collins et al., 2012 |
| Promotes overbank flow and connectivity to the floodplain | Jeffries et al., 2003; Sear et al., 2010 |

The aforementioned ways in which LW alters channel morphology all individually have the potential to impact HEF (Figure 1). These impacts on HEF have been quantitatively assessed through the use of dye, temperature, and electrical resistivity (Westhoff et al., 2011; Fox et al., 2016; Sparacino et al., 2019). HEF is primarily driven by pressure gradients, hyporheic area, and hydraulic conductivity (Gooseff et al., 2006; Buffington and Tonina, 2009). As an obstacle itself, driving flow towards the bed and banks, LW increases pressure gradients (Sawyer et al., 2011). Channel-spanning features affect HEF more than partially spanning features (Hester and Doyle,

2008, Sawyer et al., 2011). Additionally, the increased scour, bed undulations, bedform complexity, and turbulence created by the presence of LW all increase pressure gradients that in turn enhance HEF (Sawyer et al., 2011). The pools and subsequent widening that occur upstream of LW increase the area of channel that is linked to the hyporheic zone. Additionally, if a channel shifts from a single channel to a multithread system, the potential area over which HEF can occur is further increased (Tonina and Buffington, 2009). Finally, the increased substrate heterogeneity has the potential to enhance HEF (Marion et al., 2009).

The importance of enhanced HEF comes in the benefits to stream health. HEF transfers nutrients, solutes, and dissolved oxygen into the subsurface, improving habitat quality for bacteria, fungi, and micro/macro invertebrates (Boulton et al., 1998). HEF also results in an upwelling of nutrient-rich hyporheic water and increases overall nutrient retention (Lautz et al., 2006; Fanelli and Lautz, 2008; Sawyer and Cardenas, 2012). HEF functions as the "liver of the river" in that it increases water-exposure time to microbial communities that degrade contaminants and improve stream health (Fanelli and Lautz, 2008). Both invertebrates and fish embryos are extremely sensitive to temperature and take refuge in the hyporheic zone, where daily temperature fluctuations are buffered (Sawyer and Cardenas, 2012; Sawyer et al., 2012a). Understanding the influence of wood on HEF is therefore necessary for effective stream restoration and management.

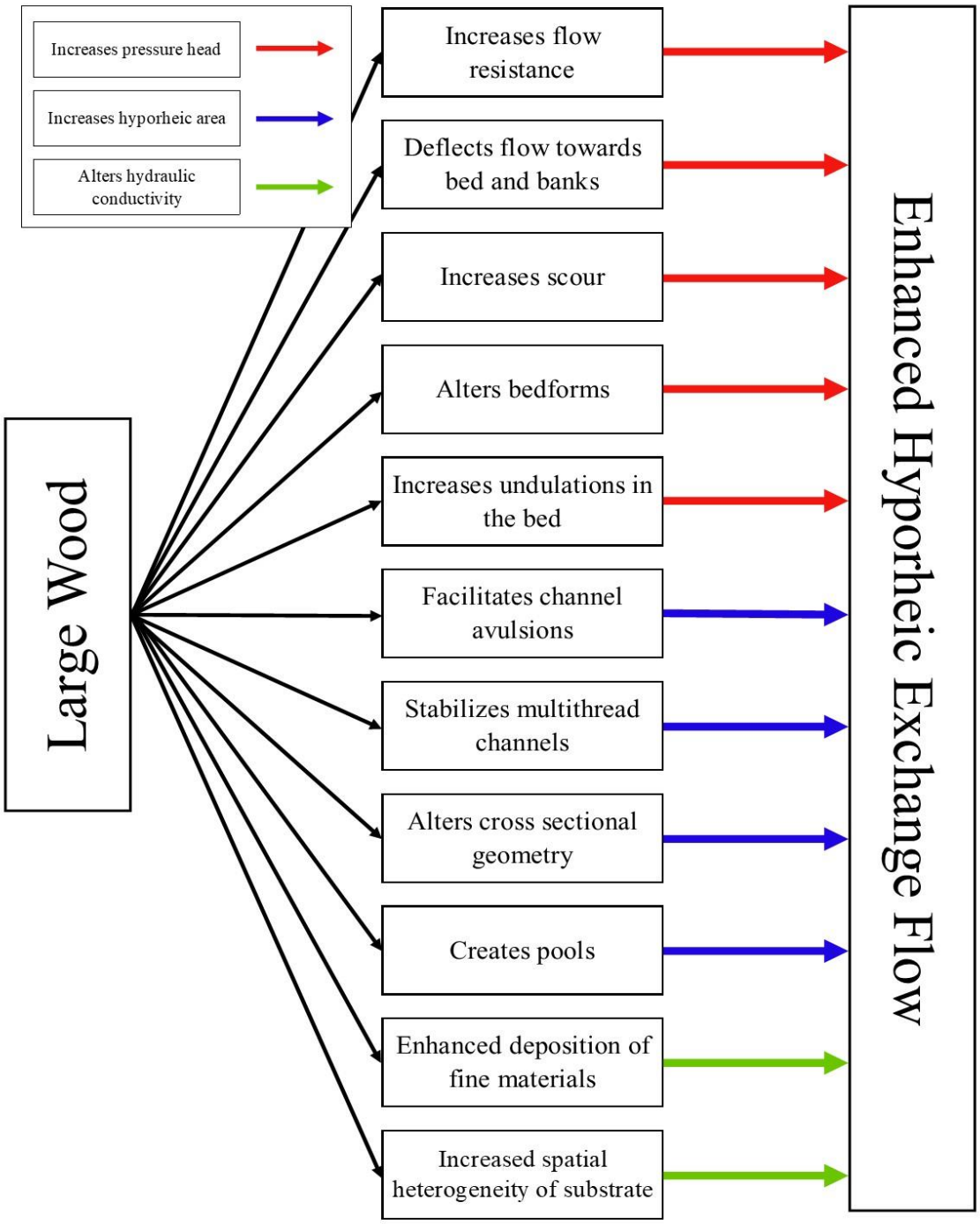


**Figure 1** - Conceptual model displaying physical impacts of LW and potential influences on HEF

While the science of hyporheic exchange has progressed over the past few decades, studies thus far have focused on single pieces of wood or single jams (e.g., Lautz et al., 2006; Sawyer et al., 2011). There have not yet been studies that examine whether multiple consecutive jams have an additive or nonlinear effect on HEF. In natural streams, it is common to have not one but multiple jams (Wohl and Beckman, 2014). Because we do not know whether multiple consecutive jams have an additive or nonlinear effect on HEF, we do not fully understand how LW influences HEF in natural streams or how to estimate minimum wood loads to create a desired magnitude of HEF in restored streams. Filling this knowledge gap will answer an important question that is relevant to all natural, forested streams and to the increasing use of engineered logjams in river restoration.

### 1.1 - Objectives and Hypotheses:

This thesis has two objectives.

Objective 1: *Analyze the relationship between increased wood loading and geomorphic complexity.*

$H1_o$: Increased wood loading does not correlate with geomorphic complexity.

$H1_a$: Increased wood loading correlates with geomorphic complexity.

In this study, geomorphic complexity will be defined by specific metrics including standard deviation of the bed elevation, substrate gradation, total sinuosity, pool volume, accumulated fine sediment volume, slope, and cross-sectional shape. A complete list of parameters used can be found in Table 3. I expect wood loading to positively correlate with these complexity metrics.

However, geomorphic complexity is also related to other factors such as valley geometry, sediment supply, riparian vegetation, and flow regime.

Objective 2: *Analyze the relationship between HEF, wood loading, and geomorphic complexity.*

$H2_o$: Increased wood loading and associated geomorphic complexity do not correlate with HEF.

$H2_a$: Increased wood loading and associated geomorphic complexity correlate with HEF.

HEF can be defined numerically in several ways including, but not limited to, hyporheic area, proportion of surface flow involved in HEF, rate of HEF, and average residence time (e.g., Haggerty et al., 2002; Wörman et al., 2002). In this study, I use the metric of skewness to represent HEF. This metric is the statistical moment of skewness for the bulk conductivity vs. time: higher values of skewness represent greater HEF. I expect HEF to increase with increased wood loading and associated geomorphic complexity. Furthermore, I examine which variables feature the strongest correlations to HEF.

## 2 - Methods

### 2.1 - Study Area

Field measurements were conducted on Little Beaver Creek (LBC), a 3$^{rd}$ order tributary to the Cache la Poudre River in the Colorado Front Range within the Arapaho and Roosevelt National Forest (Figure 2). LBC is located within the montane region at an elevation of ~2500 m. The predominant vegetation along the creek is old-growth riparian forest dominated by

ponderosa pine (*Pinus ponderosa*), aspen (*Populus tremuloides*), Engelmann spruce (*Picea engelmannii*), Douglas-fir (*Pseudotsuga menziesii*), and willows (*Salix spp.*). LW is prevalent throughout the entirety of LBC (Jackson and Wohl, 2015). LW is primarily recruited into the channels via bank erosion and individual tree fall, as there is no evidence of debris flows or landslides. This study site has evidence of past beaver presence, most notably in the form of an abandoned beaver pond formed from a dammed groundwater seep located ~20 m off channel. The hydrological regime consists of a snowmelt driven system with frequent convective summer storms. Peak bankfull flow is 0.04 $m^3/s$ and LBC has a drainage area of 37 $km^2$ (https://streamstats.usgs.gov/ss/). The mean annual rainfall of the montane region of the Colorado Front Range is 55 cm, with a mean annual temperature of 5.6° C (Barry, 1973). The underlying geology of the Colorado Front Range consists of Precambrian gneiss, granite and schist uplifted during the Laramide orogeny (Veblen and Donnegan, 2005).

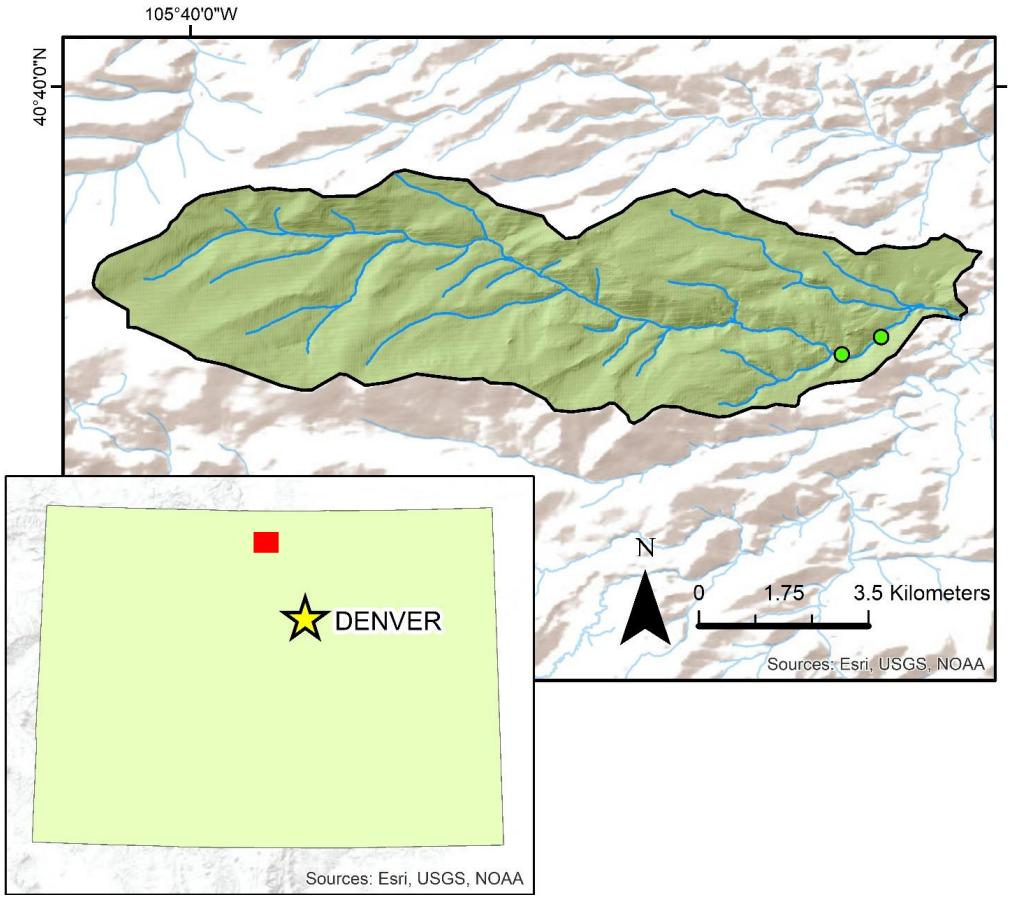


**Figure 2** - Map of Little Beaver Creek. Dots represent the upper and lower limit of the study area.

### 2.2 - Reach Selection

To examine relations among wood load, channel geometry, and HEF, I selected four reaches within 1 km on LBC: Reach 1, a single channel with no logjams, Reach 2, a single channel with limited logjams, Reach 3, an anabranching channel with limited logjams, and Reach 4, an anabranching channel with abundant logjams (Figure 3). I define "limited jams" as having downstream spacing between individual jams of greater than or equal to three times bankfull width apart and "abundant jams" as jams spaced closer than three times bankfull width.

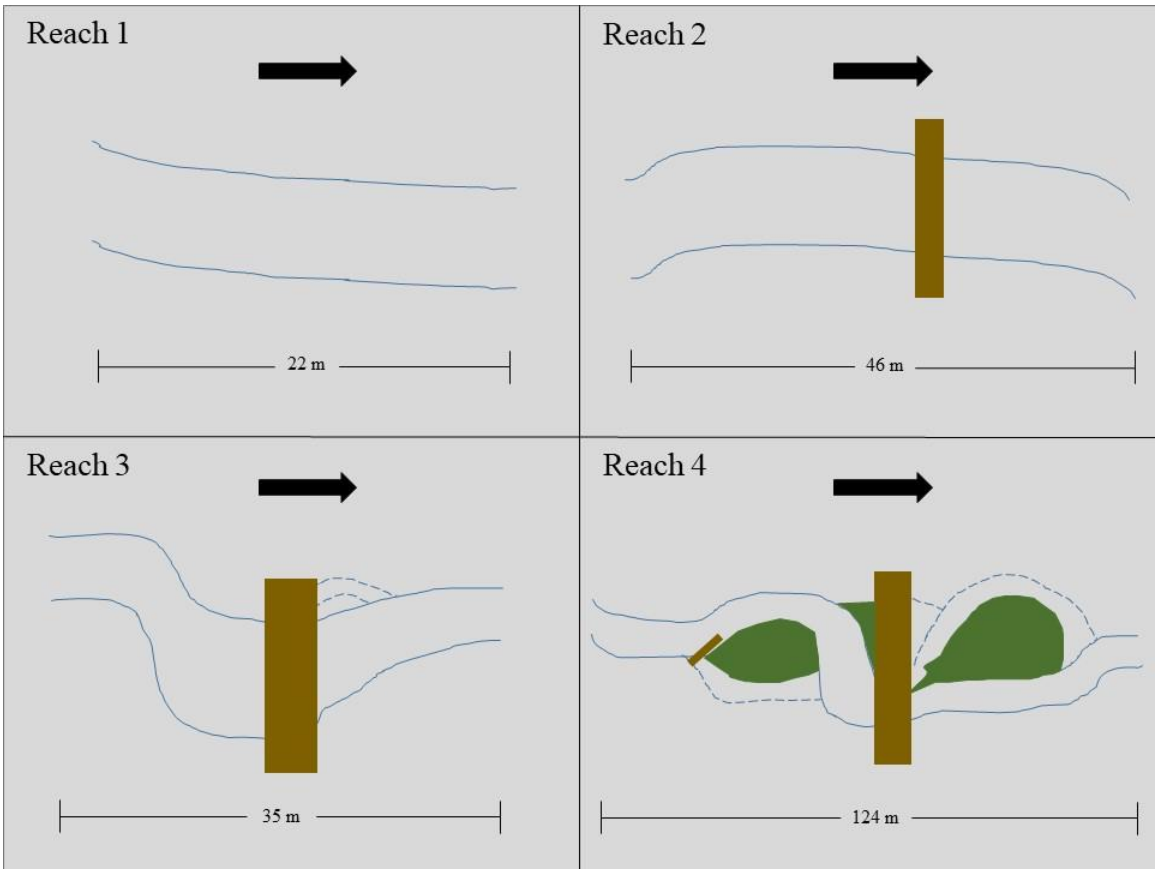


**Figure 3** - Planform schematic of four study reaches. Arrows signify flow direction, dashed lines signify side channels. Relative size of the brown bars indicates wood volume at each jam. See Figure 4 for location of all LW in the study area.

The number of study reaches was limited by the integration of the field-based geomorphic data collection with field-based salt tracer tests and electrical resistivity instrumentation used to image HEF. The tracer tests are extremely labor-intensive and time-consuming and hence constrained the number of study reaches that could be examined.

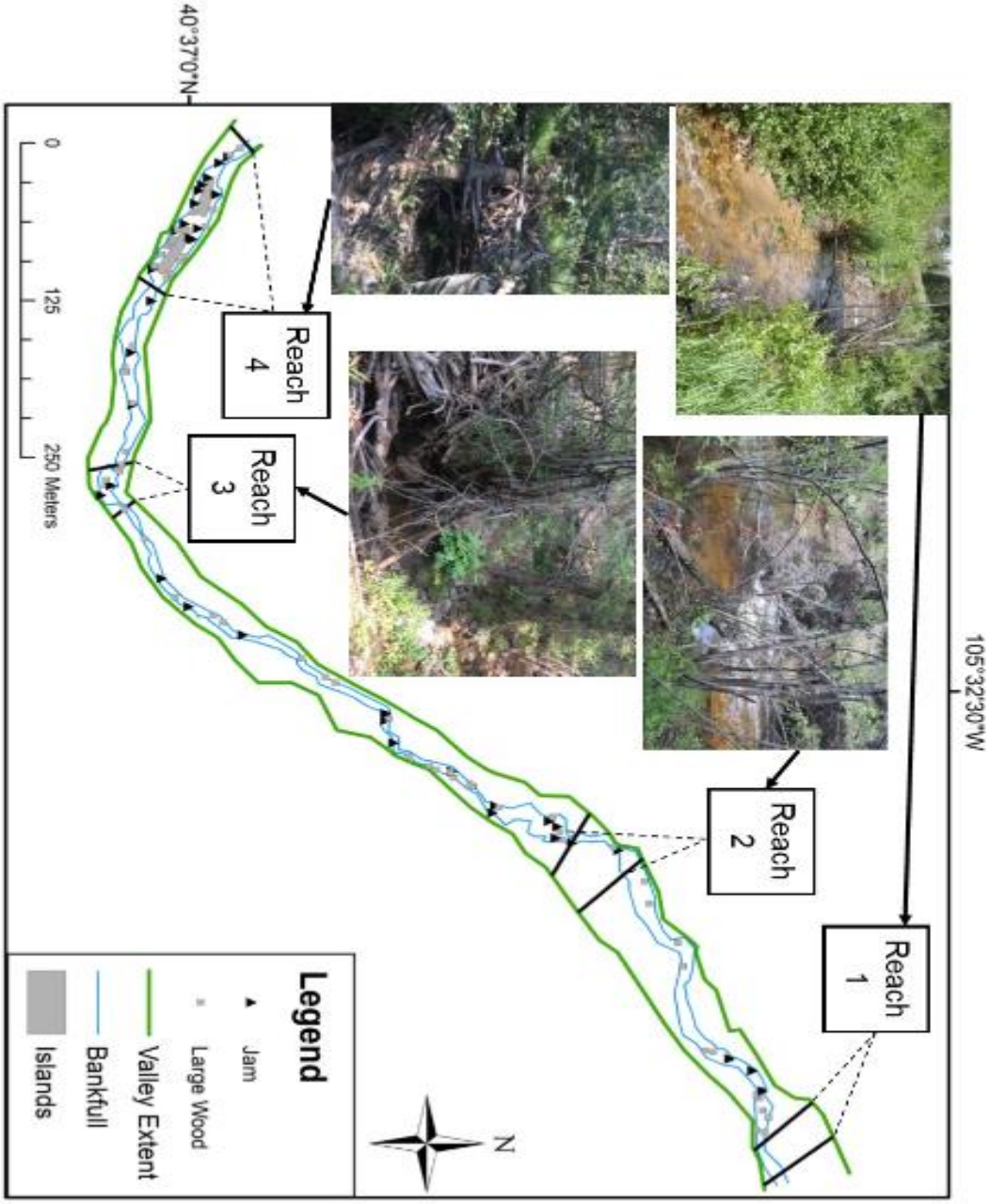


**Figure 4 -** Reach map of Little Beaver Creek with locations of all jams and individual pieces of LW

## 2.3 - Wood Variables

A continuous survey of LW was recorded walking from the most downstream point of Reach 1 to the upstream most point of Reach 4. LW is defined as any piece of wood that has a diameter exceeding 10 cm and an in-channel length exceeding 1 m. The cumulative distance traveled upstream to each successive piece of LW was measured with either a 50 m tape measurer or a Laser Technology TruPulse 360° B laser rangefinder (± 0.10 m accuracy). The diameter and in-channel length were recorded for all pieces of LW using a hand tape and a 50 m tape measurer. The volume of each piece of LW was calculated using the formula for the volume of a cylinder. The stability, level of decay, and orientation of each piece of LW was recorded. Definitions of these categorical characteristics can be found in Table 2. The latitude and longitude of each piece of LW was recorded using a Garmin eTrex 10 GPS (± 3 m accuracy). LBC is located within a laterally confined valley and it was often difficult to get a signal. Scenarios where the GPS was unable to achieve 3 m accuracy were recorded with an asterisk.

The cumulative distance traveled upstream was also recorded for jams. A jam is defined as a grouping of three or more pieces of LW that touch. A jam was classified as channel spanning if it completely spanned the bankfull channel and partially spanning if the jam only occupied a portion of the channel. All of the same measurements and classifications previously defined for LW were used for the key piece of each jam. The key piece is defined as the piece of LW that provides the most structural integrity to the jam. Each additional piece of LW in the jam was defined as Other 1, Other 2, etc. The diameter and in-channel length was recorded for each "Other" piece of wood. Jams commonly contained a considerable amount of wood and detritus that was too small to be considered LW. A rectangular prism that encompassed this remaining portion of the jam was visually estimated and the length, width, and height were measured using

a 50 m tape measure or a stadia rod. Furthermore, the porosity (p) of this rectangle was visually estimated because the degree of permeability could influence the magnitude of the pressure head. The volume of wood within this rectangle is therefore equal to:

$$V = L \times W \times H \times (1 - p)$$

This volume, when combined with the volume of the key piece and other pieces yields the total volume of the jam. The total volume of each jam is a minimum estimate of the true volume as there are inevitably pieces that are buried and pieces that are too small to measure.

The length, width, and depth of pools related to the jams were measured if present using a stadia rod. The pools were estimated to be rectangular prisms in which depth extended from the riverbed up to bankfull stage. The pools were classified as either backwater or plunge pools. Where present, sediment finer than the average channel substrate was measured upstream of the jam. The sediment accumulations were estimated to be rectangular prisms in all but one case where the sediment accumulation took the shape of a triangular prism. A stadia rod was used to measure the length and width of the sediment accumulation while a piece of rebar was probed into the accumulation to obtain the depth.

**Table 2 - Categorical characteristics of LW**

| Category | Classification | Description |
|---|---|---|
| Stability | Unattached | The piece of LW lies loosely in the channel |
| | Bridge | Both ends of LW rest upon opposing banks, propping piece above the channel |
| | Ramp Left/Right | One end of LW sits on river left or river right bank, while the other end rests in the channel |
| | Pinned | Piece of LW is held in place in at least one spot by boulders or another piece of wood |
| | Buried | Part of LW piece is buried in the channel. Pieces can be both buried and a ramp left/right or pinned |
| Root Wad | Yes/No | Does the piece of LW have a root wad attached |
| Decay | D1 | Piece still has its bark, small branches, and needles |
| | D2 | Piece has lost its needles and smaller branches |
| | D3 | Piece has lost a significant portion of its bark |
| | D4 | Piece is rotten to the point that pieces can be pulled back by hand |
| | Alive | Piece is a part of a tree that is still alive |
| Orientation | Parallel | Piece is oriented parallel to the flow direction |
| | Perpendicular | Piece is oriented perpendicular to the flow direction |
| | Oblique | The piece is oriented between parallel and perpendicular |

## 2.4 - Geomorphic Variables

Five valley cross sections were taken in each reach. The selection of cross sections within each reach attempted to evenly space the cross sections while also minimizing the disturbance to local vegetation. Cross sectional distance from right valley-bottom edge was measured with a metric tape and elevation was measured using a laser rangefinder. Significant geomorphic features noted during the survey included, but were not limited to bankfull right, bankfull left, water's edge, cut banks, and the thalweg. Bankfull was indicated by clear breaks in slope and occasionally by changes in vegetation. The locations of the start and end point of each cross section were recorded using a GPS. These valley cross sections were used to obtain the average valley width of each cross section. Additionally, the portions of the cross sections that encompassed the channel were used to determine average bankfull width, bankfull depth, and cross sectional area for each reach. All five cross sections were used in these averages in reaches 1, 2, and 4. Only three valley cross sections were used in these calculations for reach 3, where the sinuosity of the valley caused two cross sections to diagonally cross the channel. While these two cross sections accurately represent the valley width, they cannot be used to accurately characterize bankfull width or cross sectional area.

A longitudinal thalweg profile was also created for the main channel of each reach and for side channels, where present. For each profile, a 100 m measuring tape, CST/Berger 24X automatic level, and stadia rod were used to survey each break in slope or every 2 m. The base of the stadia rod always stood on the bed in the thalweg except when major jams were present. Stadia rod readings were taken at the base of the jam, on top of the jam, and upstream of the jam. The readings taken on top of the jams were not used in calculating bed slope or the undulations

of the bed. The undulations of the bed were calculated from the standard deviation of the residuals of the longitudinal profile when regressed (Yochum et al., 2012).

GPS points were taken along bankfull right and left as well as along the extent of valley right and left. These points were used to obtain the total sinuosity of the channel using the distance function in ArcGIS ver 10.5.

A sediment distribution was created for the main channel of each reach and, where present, side channel. The sediment distributions were created by randomly selecting and measuring 100 clasts in a representative location within the channel. The grain size of each clast was determined by using a gravelometer. A classification of sand or silt was visually assigned to clasts smaller than 4 mm and a boulder was anything greater than 256 mm. These data were used to determine the d16, d50, d84, and gradation coefficient for each reach. Additionally, a 50 m measuring tape was laid in the middle of the channel. At each meter marking, a clast was measured from river right, the middle of the channel, and river left.

**2.5 - Subsurface Variables**

Daniel McGrath of the Department of Geosciences at Colorado State University oversaw two ground penetrating radar (GPR) transects using a pulseEKKO® PRO control unit with a 200 MHz antenna. A cross-sectional transect was taken through both Reaches 1 and 4 with traces being taken every 10 cm.

HEF was measured using electrical resistivity (ER). These data were obtained under the supervision of Megan Doughty, Jackie Randall, and Kamini Singha from Colorado School of Mines (CSM). ER was collected using an IRIS Syscal Pro Resistivity Meter during constant-rate tracer injections of dissolved NaCl. Tracer was injected into the middle of the stream for four

hours for each measurement and ER was monitored for a minimum of 24 hours post injection. We assume that complete mixing of the tracer into the stream occurs.

The ER data come from 4 tracer tests; one each on June 13th (reaches 1 and 2, 0.76 cms), July 10th (reaches 1 and 2, 0.17 cms), July 28th (reaches 1 and 2. 0.18 cms), and July 30th (reach 4, 0.18 cms) (Doughty, 2019). I do not use the peak flow (June 13) data in this thesis because this test did not involve the reaches with multiple logjams. I use data from the tests on July 10th and July 30th to compare reaches 1, 2, and 4 because these tests have comparable discharges. I use the July 10th results in place of the July 28th tracer test because a thunderstorm disrupted the July 28th collection, altering the results. Megan Doughty and Sawyer McFadden at CSM inverted these data to obtain skewness values for reaches 1, 2, and 4.

The statistical moment of skewness represents the symmetry of a distribution and is used in this study as a proxy for the rate of HEF. Skewness can be used to show relative increases in HEF i.e. twice as much skewness does not imply twice as much HEF. Figure 5a displays a scenario in which the tracer exits the system at the same rate as it entered. In this case, no HEF occurs and skewness is 0. In 5b, the tracer enters the hyporheic zone and is retained in the system for a longer period of time, skewing the distribution to the right. Distributions with higher values of skewness exhibit greater amounts of HEF. A model created to represent processes at Little Beaver Creek utilized a hydraulic conductivity value of 8 m/d (Doughty, 2019).

**2.6 - Statistical Methods**

The intensive data collection and single field season limited the number of study reaches. With such a small sample size (n=4 for Objective 1, n=3 for Objective 2), most statistical methods including but not limited to a multiple linear regression model are inappropriate to use.

Simple linear correlations such as the Pearson correlation are the only appropriate statistical tools. Therefore, most relationships have been qualitatively assessed.

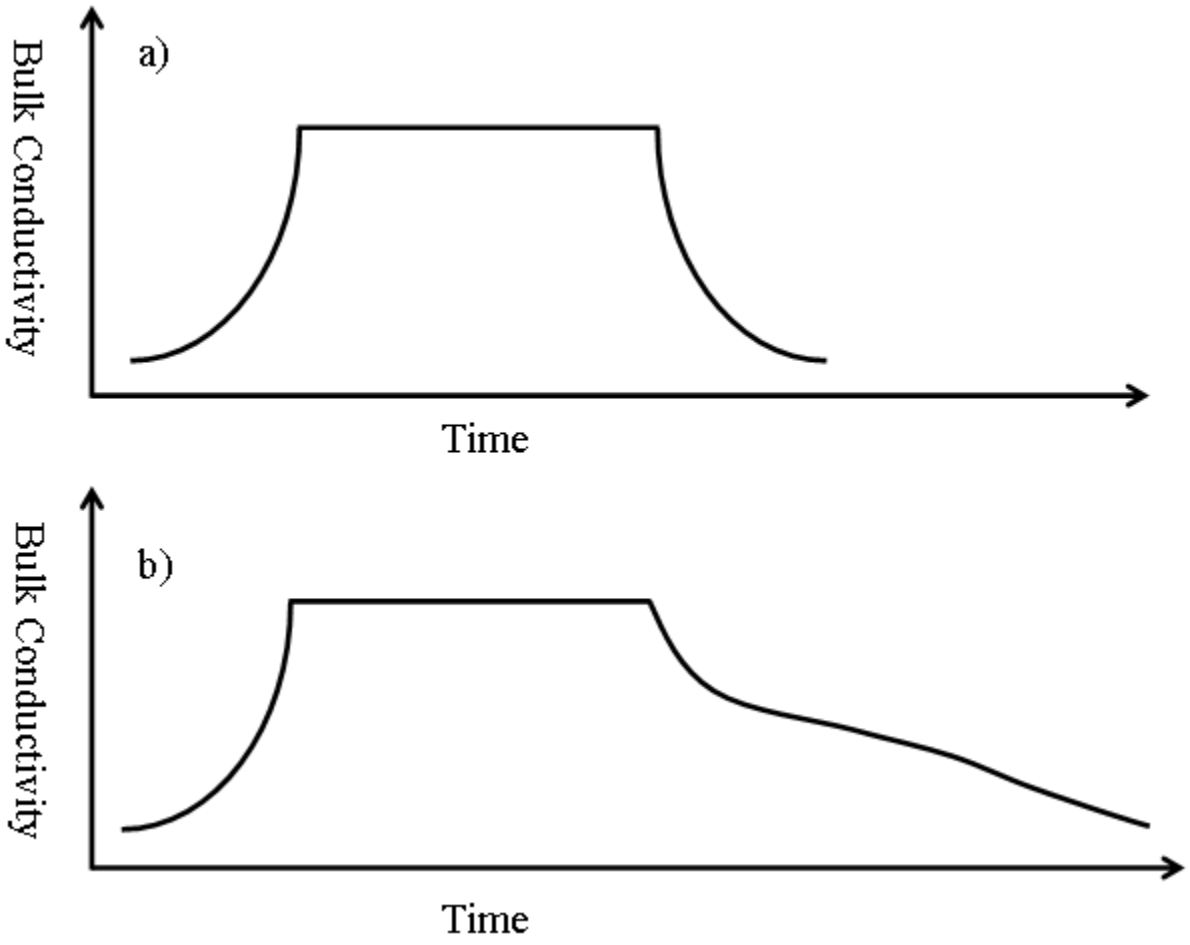


**Figure 5 -** Conceptual drawing of HEF distributions when a) skewness is 0 and b) skewness is positive

**Table 3 - Summary of all parameters used in statistical analysis**

| Parameter (Units) | Description |
|---|---|
| d50 (mm) | The median grain size |
| Gradation coefficient (dimensionless) | Gradation of the grain size distribution; $\frac{1}{2}(\frac{d_{84}}{d_{50}} + \frac{d_{50}}{d_{16}})$ |
| Average bankfull width (m) | Reach averaged bankfull width |
| Average bankfull depth (cm) | Reach averaged bankfull depth |
| Width to depth ratio (dimensionless) | Ratio of average bankfull width to average bankfull depth |
| Average cross sectional area ($m^2$) | Reach averaged cross sectional area |
| Slope (dimensionless) | Reach averaged bed slope |
| Average Valley Width (m) | Reach averaged valley width |
| Yochum $\sigma_z$ (m) | Standard deviation of the residuals of a regressed longitudinal profile |
| Total Sinuosity (dimensionless) | Total channel length per reach, side channels included, normalized by valley length |
| Normalized total pool volume ($m^2$) | Total volume of pools per reach normalized by valley length |
| Normalized total fines volume ($m^2$) | Total volume of accumulated fine sediment per reach normalized by valley length |
| Normalized total wood volume ($m^2$) | Total volume of both LW and jams per reach normalized by valley length |
| Skewness (dimensionless) | Proxy for rate of HEF. Statistical moment of skewness for the solute concentration vs. time |

## 3 - Results and Discussion

Preliminary GPR results suggest that the depth to bedrock is greater at reach 1 (~2-3 m) vs. reach 4 (~1 m). The June 13$^{th}$ tracer test shows that reach 2, a single channel with limited jams, yields a higher skewness than reach 1, a single channel with no jams (225 vs. 204). Table 4 presents a basic summary of the sample size and mean or total values for field measured variables.

**Table 4 - Summary of field data with sample size of collection**. Skewness data for reaches 1 and 2 come from the July 10th tracer test and skewness data for reach 4 come from the July 30th tracer test.

| Reach | 1 | 2 | 3 | 4 |
|---|---|---|---|---|
| **Geomorphic** | | | | |
| d50 (mm) | 45<br>n = 100 | 60<br>n = 100 | 45<br>n = 100 | 60<br>n = 100 |
| Gradation coefficient | 2.41<br>n = 100 | 2.4<br>n = 100 | 2<br>n = 100 | 2.4<br>n = 100 |
| Channel Length (m) | 22 | 47 | 38.8 | 124.6 |
| Valley Length (m) | 20 | 42 | 25.5 | 105 |
| Bankfull width (m) | 4.7<br>n = 5 | 5.6<br>n = 5 | 7.5<br>n = 3 | 8.9<br>n = 5 |
| Bankfull depth (cm) | 50<br>n = 5 | 57<br>n = 5 | 53<br>n = 5 | 60<br>n = 5 |
| Width to depth ratio | 9.4 | 9.9 | 14.2 | 14.9 |
| Cross sectional area ($m^2$) | 1.67<br>n = 5 | 2.45<br>n = 5 | 2.48<br>n = 3 | 4.2<br>n = 5 |
| Slope | 0.022 | 0.022 | 0.029 | 0.034 |
| Valley Width (m) | 55<br>n = 5 | 49<br>n = 5 | 27<br>n = 5 | 23<br>n = 5 |
| Yochum $\sigma_z$ (m) | 0.12 | 0.08 | 0.19 | 0.16 |
| Total Sinuosity | 1.1 | 1.1 | 1.65 | 1.81 |
| **Wood** | | | | |
| LW volume ($m^3$) | 0<br>n = 0 | 0.03<br>n = 1 | 0.66<br>n = 9 | 1.15<br>n = 21 |
| Jam volume ($m^3$) | 0<br>n = 0 | 3.21<br>n = 2 | 9.78<br>n = 2 | 11<br>n = 13 |
| Total wood volume ($m^3$) | 0 | 3.23 | 10.45 | 12.51 |
| Total pool volume ($m^3$) | 0<br>n = 0 | 2.39<br>n = 1 | 32.49<br>n = 2 | 9.06<br>n = 2 |
| Total fines volume ($m^3$) | 0<br>n = 0 | 0.61<br>n = 1 | 9.62<br>n = 1 | 2.52<br>n = 3 |
| **HEF** | | | | |
| Skewness | 120<br>n = 1 | 185<br>n = 1 | NA | 380<br>n = 1 |

### 3.1 – Hypothesis 1

Observations in this section are drawn from a dataset with a sample size of four. Therefore, the discussion mainly consists of qualitative conclusions. Table 5 summarizes the

results of the Pearson correlations against normalized total wood volume. Meaningful relationships are displayed in Figure 6.

**Table 5 - $r^2$ values from Pearson correlations between geomorphic parameters and wood volume.** Bolded parameters are interpreted as physically meaningful.

| Response variable correlated vs. normalized total wood volume | Pearson $r^2$ | Direction of Correlation |
|---|---|---|
| **Normalized total pool volume** | **0.92** | **+** |
| **Normalized total fines volume** | **0.92** | **+** |
| Gradation coefficient | 0.89 | - |
| **Yochum $\sigma_z$** | **0.63** | **+** |
| Average valley width | 0.52 | - |
| Width to depth ratio | 0.50 | + |
| Total Sinuosity | 0.41 | + |
| Average bankfull width | 0.32 | + |
| Slope | 0.29 | + |
| d50 | 0.07 | + |
| Average cross sectional area | 0.04 | + |
| Average bankfull depth | 0.00 | NA |

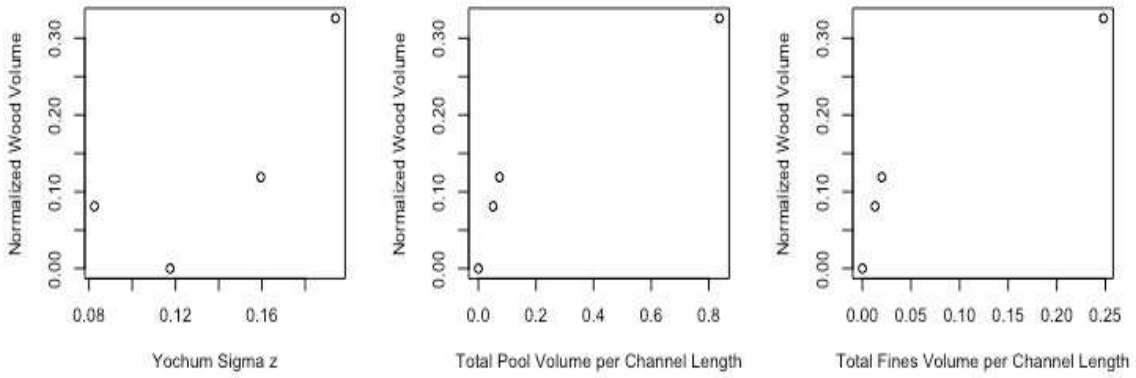


**Figure 6** - Plots of meaningful relationships between geomorphic parameters and wood volume

Although the gradation coefficient features a strong correlation to normalized total wood volume, the values only range from 2.0 to 2.4. The grain size distributions for the four reaches,

which were collectively within a kilometer of one another, were extremely similar and will not be discussed further.

The two parameters that have the strongest positive correlations to normalized total wood volume are the normalized total pool volume and the normalized total volume of fine sediments ($r^2 = 0.92$). Reaches with more wood had both more pools and larger pools. The pools and associated fine sediments mainly occurred at the largest jam in each reach. No individual pieces of LW created any pools or accumulated fines within any of the four reaches. Reach 3 had the largest jam in the system and consequently a larger backwater effect. The scour and turbulence caused by the blockage of the jam increases pool volume while the decreased velocities immediately upstream of the jam lead to an accumulation of fine materials. Both of the largest jams in reaches 3 and 4 consisted of large trees that fell perpendicularly across the channel with root wads still embedded in the banks. Wood recruitment via undercutting of the banks seems to be the process that creates the largest jams. A large piece of LW with a decay classification of D1 lay parallel to the stream in the pool immediately upstream of the main jam in reach 3. This piece of LW helped retain sediment in the pool as the smaller branches and needles likely shielded the sediment from flow.

The standard deviation of the bed elevation also shows a positive correlation to normalized total wood volume ($r^2 = 0.63$). This relationship supports previous research (e.g., Keller and Swanson, 1979; Brummer et al., 2006) and also suggests a positive feedback loop. The presence of LW increases heterogeneity of entrainment and deposition, which increases the size and frequency of undulations in the bed surface. However, these breaks in slope also aid the retention and deposition of LW (Braudrick and Grant, 2001).

### 3.2 - Hypothesis 2

Observations in this section are drawn from a sample size of three. Therefore, as in the previous section, this discussion consists of qualitative conclusions. Table 6 summarizes the results of the Pearson correlations against skewness. Meaningful relationships are displayed in Figure 7.

**Table 6 - $r^2$ values from Pearson correlations between geomorphic parameters, wood loading, and skewness.** Bolded parameters are interpreted as meaningful. The nature of the potential impact on HEF is represented by an x in the final three columns.

| Predictor variable correlated vs. skewness | Pearson $r^2$ | Direction of Correlation | PH[1] | HA[1] | HC[1] |
|---|---|---|---|---|---|
| **Average bankfull width** | **1.00** | **+** | | x | |
| **Average cross sectional area** | **1.00** | **+** | | x | |
| Average valley width | 0.99 | - | | x | |
| **Width to depth ratio** | **0.98** | **+** | | x | |
| **Slope** | **0.97** | **+** | x | | |
| **Total sinuosity** | **0.94** | **+** | | x | |
| **Normalized total fines volume** | **0.81** | **+** | | | x |
| **Normalized total wood volume** | **0.78** | **+** | x | | |
| **Normalized total pool volume** | **0.76** | **+** | | x | |
| Average bankfull depth | 0.76 | + | | | |
| Yochum $\sigma_z$ | 0.57 | + | x | | |
| d50 | 0.48 | + | | | x |
| Gradation coefficient | 0.48 | - | | | x |

[1] Pressure head (PH), hyporheic area (HA), hydraulic conductivity (HC)

Although average valley width correlates strongly with skewness, the correlation is inverse. Reach 4, which yielded the highest skewness and therefore had the highest rate of HEF, was also the most confined reach with an average valley width of only 23 m versus 55 m and 49 m for reaches 1 and 2, respectively. We expected less confined valley segments to equate to greater potential for HEF to penetrate laterally into the banks, but our results did not support this expectation. There is more than one potential explanation for the inverse correlation between valley width and HEF. Little Beaver Creek is snowmelt-dominated and unlikely to have extreme

floods that might include sufficient flow volume to create HEF across the entire width of a wider valley segment. I do not know the subsurface distribution of sediments with limited permeability, which might be present and limit the extent of HEF. Consequently, I posit that valley width may serve as a limiting factor rather than a predictor of HEF. The fact that reach 4 has the greatest HEF despite having the narrowest valley width and shallowest depth to bedrock could also reflect the strong influence of the jams and other wood-related geomorphic features on HEF.

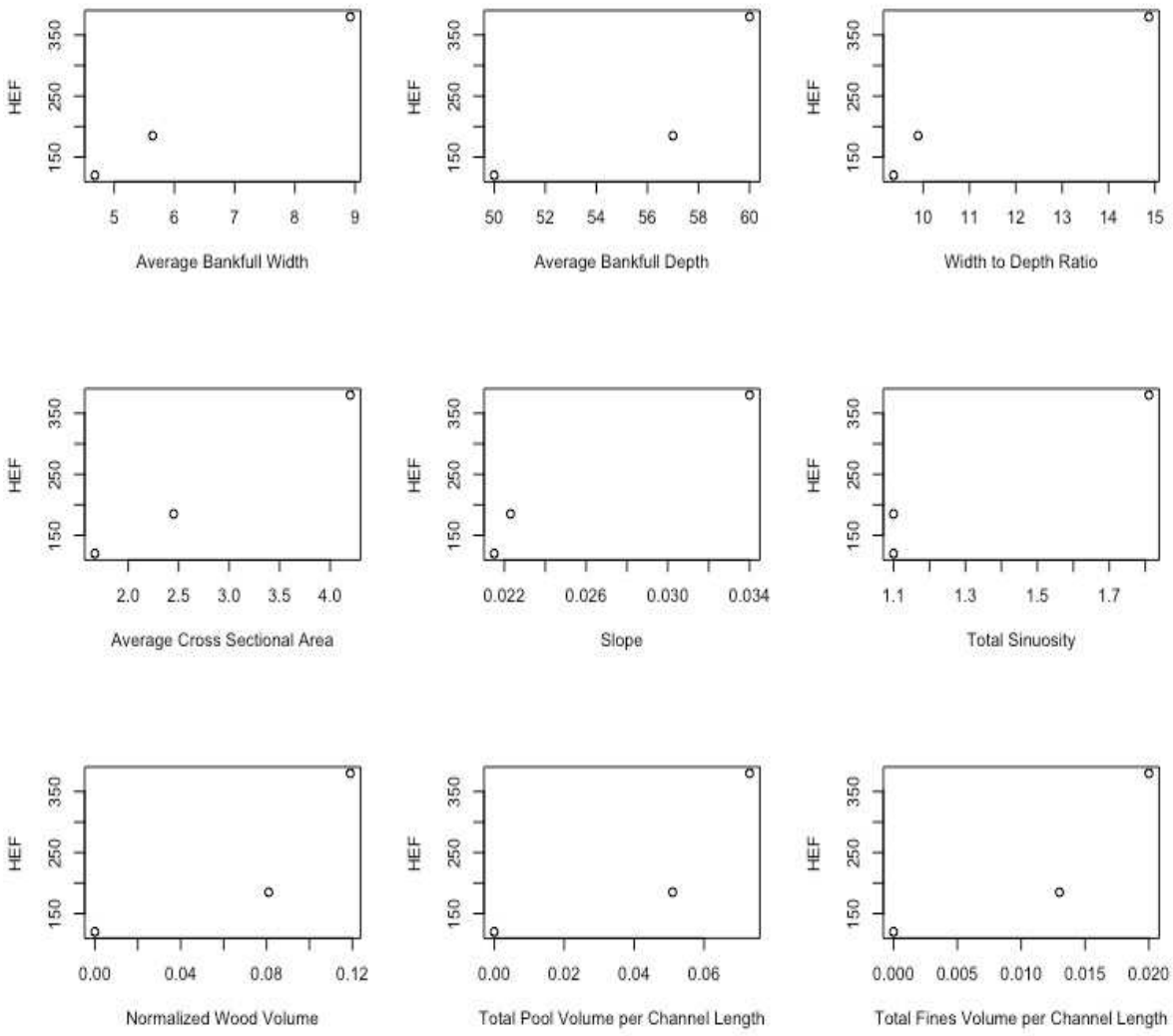


**Figure 7** - Plots of meaningful relationships between geomorphic parameters, wood loading, and skewness

Average bankfull width, average cross sectional area, width to depth ratio, and total sinuosity all have very strong positive correlations to skewness ($r^2 \geq 0.94$). A greater bankfull width, average cross sectional area, width to depth ratio, and total sinuosity all increase the connectivity from the channel to the hyporheic zone. This increased access to the hyporheic zone increases the potential for a larger hyporheic area, and therefore increases rates of HEF. Increased connectivity to the hyporheic zone in reach 4 likely primarily reflects the multichannel planform. The multichannel planform also numerically manifests itself in the higher value of total sinuosity in reach 4.

Slope also has a strong positive correlation to skewness ($r^2 = 0.97$). Having a greater bed slope amplifies the magnitude of the pressure gradients, which in turn increases the rate at which HEF can occur (Tonina, 2005). Normalized total wood volume shows a weaker positive correlation to skewness ($r^2 = 0.78$). Increased wood loading also increases the pressure gradients by driving flow towards the bed and banks. Similar correlations exist for normalized total fines volume and normalized total pool volume ($r^2 = 0.81, 0.76$). The analysis for Hypothesis 1 shows that volumes of wood, fine sediments, and pools are all very closely correlated. This explains why they all have a similar correlation to skewness. Because jams in reach 4 were taller than jams in reach 2, I would expect them to have a greater impact on pressure head and connectivity from the channel to the hyporheic zone.

Having a greater volume of accumulated fines on the bed surface increases the vertical heterogeneity of sediment, which has the potential to increase HEF. Having a greater pool volume increases spatial connectivity to the hyporheic area (Buffington and Tonina, 2009).

## 4 - Conclusions

Although increased wood load does not strongly correlate with all metrics representing geomorphic complexity, it does increase the volume of both pools and accumulated fine sediment at the reach level. HEF did positively correlate with geomorphic complexity and wood loading. The metrics that most strongly correlated with enhanced HEF all represent factors expected to increase connectivity from the channel to the hyporheic zone. These preliminary results suggest that it is through this mechanism of increasing hyporheic zone connectivity that HEF is enhanced rather than through the mechanisms of increasing pressure head or altering hydraulic conductivity. Future work will increase the sample size, allowing for a linear regression analysis, which will provide a stronger answer to objective 2. Increased wood loading does enhance HEF, which in turn improves stream health. This provides another reason for managers to implement LW in river restoration designs.

### 4.1 – Future Work

The work from this thesis has been the first of a three-year National Science Foundation-funded project. Future work will involve two more seasons of field work, the first of which will more closely analyze HEF in the more complex reaches 3 and 4. A flume study will be carried out at Colorado State University and a numerical model will be developed at Ohio State University. These models, both physical and numerical, will help answer more specific questions about HEF such as:

1) Which geomorphic features are the strongest predictors on HEF?

1) Does increased wood loading have an additive or nonlinear effect on HEF?

**References**


Abbe, T.B., Brooks, A.P., Montgomery, D.R., 2003. Wood in river rehabilitation and management. In: Gregory, S.V., Boyer, K.L., Gurnell, A.M. (Eds.), The Ecology and Management of Wood in World Rivers. American Fisheries Society, Bethesda, MD, pp. 367–389.

Barry, R.G., 1973. A climatological transect on the east slope of the Front Range, Colorado. Artic Antarctic and Alpine Research 5, 89– 110.

Beschta R.L., 1983. The effects of large organic debris upon channel morphology: a flume study. In, Proceedings of the D.B. Simons Symposium on Erosion and Sedimentation, Fort Collins, CO, pp. 8-63 to 8-78.

Bocchiola, D., 2011. Hydraulic characteristics and habitat suitability in presence of woody debris: a flume experiment. Advances in Water Resources 34, 1304–1319.

Boulton, A.J., et al., 1998. The functional significance of the hyporheic zone in streams and rivers. Annual Review of Ecology and Systematics 29, pp. 59–81.

Braudrick, C.A., Grant, G.E., 2001. Transport and deposition of large woody debris in streams: a flume experiment. Geomorphology 41, 263-283.

Brummer, C.J., Abbe, T.B., Sampson, J.R., Montgomery, D.R., 2006. Influence of vertical channel change associated with wood accumulations on delineating channel migration zones, Washington, USA. Geomorphology 80, 295-309.

Buffington, J.M., Montgomery, D.R., 1999. Effects of hydraulic roughness on surface texture of gravel-bed rivers. Water Resources Research 35, 2507-3521.

Buffington, J.M., Tonina, D., 2009. Hyporheic exchange in mountain rivers II: effects of channel morphology on mechanics, scales, and rates of exchange. Geography Compass 3.

Cherry, J., Beschta, R.L., 1989. Coarse woody debris and channel morphology: a flume study. Water Resources Bulletin 25, 1031–1036.

Collins, B.D., Montgomery, D.R., Fetherston, K.L., Abbe, T.B., 2012. The floodplain large wood cycle hypothesis: a mechanism for the physical and biotic structuring of temperate forested alluvial valleys in the North Pacific coastal ecoregion. Geomorphology 139-140, 460–470.

Curran, J.H., Wohl, E., 2003. Large woody debris and flow resistance in step-pool channels, Cascade Range, Washington. Geomorphology 51, 141–157.

Daniels, M.D., Rhoads, B., 2004. Effect of large woody debris configuration on three dimensional flow structure in two low-energy meander bends at varying stages. Water Resources Research 40, W11302. http://dx.doi.org/10.1029/2004WR003181.

Davidson, S.L., Eaton, B.C., 2013. Modeling channel morphodynamic response to variations in large wood: implications for stream rehabilitation in degraded watersheds. Geomorphology 202, 59–73.

Doughty, M., 2019. Electrical imagining of hyporheic exchange from channel-spanning logjams.. Unpublished MS thesis. Golden, CO: Colorado School of Mines

Fanelli R.M., Lautz L.K., 2008. Patterns of water, heat, and solute flux through streambeds around small dams. Groundwater 46: 671-687.

Faustini, J.M., Jones, J.A., 2003. Influence of large woody debris on channel morphology and dynamics in steep, boulder-rich mountain streams, western Cascades, Oregon. Geomorphology 51, 187–205.

Fox, A., Laube, G., Schmidt, C., Fleckenstein, J.H., Arnon, S., 2016. The effect of losing and gaining flow conditions on hyporheic exchange in heterogeneous streambeds. Water Resources Research 52, 7460-7477.

Gendaszek, A.S., Magirl, C.S., Czuba, C.R., 2012. Geomorphic response to flow regulation and channel and floodplain alteration in the gravel-bedded Cedar River, Washington, USA. Geomorphology 179, 258–268.

Haggerty, R., Wondzell, S.M., Johnson, M.A., 2002. Power-law residence time distribution in the hyporheic zone of a 2nd-order mountain stream. Geophysical Research Letters 29, 1640, 10.1029/2002GL014743.

Hester, E.T., Doyle, M.W., 2008. In-stream geomorphic structures as drivers of hyporheic exchange, Water Resources Research 44, W03417, doi:10.1029/2006WR005810.

Jackson, K.J., Wohl, E., 2015. Instream wood loads in montane forest streams of the Colorado Front Range, USA. Geomorphology 234, 161-170.

Jeffries, R., Darby, S.E., Sear, D.A., 2003. The influence of vegetation and organic debris on flood-plain sediment dynamics: case study of a low-order stream in the New Forest, England. Geomorphology 51, 61-80.

Keller, E.A., Swanson, F.J., 1979. Effects of large organic material on channel form and fluvial processes. Earth Surface Processes 4, 361–380.

Lautz, L.K., Siegel, D.I., Bauer, R.L., 2006. Impact of debris dams on hyporheic interaction along a semi-arid stream. Hydrological Processes 20, 183–196.

MacFarlane, W.A., Wohl, E., 2003. Influence of step composition on step geometry and flow resistance in step-pool streams of the Washington Cascades. Water Resources Research 39. http://dx.doi.org/10.1029/2001WR001238.

Manga, M., Kirchner, J.W., 2000. Stress partitioning in streams by large woody debris. Water Resources Research 36, 2373–2379.

Marion, A., Packman, A.I., Zaramella, M., Bottacin-Busolin, A., 2008. Hyporheic flows in stratified beds. Water Resources Research 44, W09433, doi:10.1029/2007WR006079

Montgomery, D.R., Buffington, J.M., 1997. Channel-reach morphology in mountain drainage basins. GSA Bulletin; 109 (5): 596–611.

Nakamura, F., Swanson, F.J., 1993. Effects of coarse woody debris on morphology and sediment storage of a mountain stream system in western Oregon. Earth Surface Processes and Landforms 18, 43–61.

O'Connor, J.E., Jones, M.A., Haluska, T.L., 2003. Flood plain and channel dynamics of the Quinault and Queets Rivers, Washington, USA. Geomorphology 51, 31–59.

Sawyer, A. H., Cardenas, M.B., Buttles, J., 2012. Hyporheic temperature dynamics and heat exchange near channel-spanning logs, Water Resources Research, 48, W01529, doi:10.1029/2011WR011200.

Sawyer, A. H., Cardenas, M.B., Buttles, J., 2011. Hyporheic exchange due to channel-spanning logs, Water Resources Research, 47, W08502, doi:10.1029/2011WR010484

Sawyer, A. H., Cardenas, M.B., 2012, Effect of experimental wood addition on hyporheic exchange and thermal dynamics in a losing meadow stream, Water Resources Research, 48, W10537, doi:10.1029/2011WR011776

Sear, D.A., Millington, C.E., Kitts, D.R., Jeffries, R., 2010. Logjam controls on channel: floodplain interactions in wooded catchments and their role in the formation of multi-channel patterns. Geomorphology 116, 305-319.

Sparacino, M.S., Rathburn, S.L., Covino, T.P., Singha, K., Ronayne, M.J., 2019. Form-based river restoration decreases wetland hyporheic exchange: Lessons learned from the Upper Colorado River. Earth Surface Processes and Landforms 44, 191-203.

StreamStats. U.S. Geological Survey website: https://streamstats.usgs.gov/ss/

Tonina, D., Buffington, J.M., 2009. Hyporheic exchange in mountain rivers I: mechanics and environmental effects. Geography Compass 3: 1063-1086.

Tonina, D., 2005. Interaction between river morphology and intra-gravel flow paths within the hyporheic zone. unpublished Ph.D. dissertation, Boise, ID: University of Idaho.

Veblen, T.T., Donnegan, J.A., 2005. Historical range of variability for forest vegetation of the national forests of the Colorado Forest Range 151 pp. Forest Service Rocky Mountain Region, U.S. Department of Agriculture, Golden, Colorado.

Wallerstein, N.P., Thorne, C.R., 2004. Influence of large woody debris on morphological evolution of incised, sand-bed channels. Geomorphology 57, 53–73.

Westhoff, M.C., Gooseff, M.N., Bogaard, T.A., Savenije, H.H.G., 2001. Quantifying hyporheic exchange at high spatial resolution using natural temperature variations along a first-order stream. Water Resources Research 47, W10508, doi:10.1029/2010WR009767.

Wohl, E., Beckman, N.D., 2014a. Controls on the longitudinal distribution of channel spanning logjams in the Colorado Front Range, USA. River Research and Applications 30, 112–131.

Wohl, E., 2011b. Threshold-induced complex behavior of wood in mountain streams. Geology 39, 587–590

Wohl, E., 2017. Bridging the gaps: an overview of wood across time and space in diverse rivers. Geomorphology 279, 3–26.

Wörman A, Packman A.I., Johansson H., Jonsson K., 2002. Effect of flow-induced exchange in hyporheic zones on longitudinal transport of solutes in streams and rivers. Water Resources Research, 38. doi:10.1029/2001WR000769.

Yochum, Bledsoe, David, & Wohl. (2012). Velocity prediction in high-gradient channels. Journal of Hydrology, 424-425(C), 84-98.

## Appendices

### Appendix A - Grain size data

**Table A1 - Grain size distributions for all four reaches and side channels**

| Size (mm) | Reach 1 count | Reach 2 count | Reach 3 count | Reach 4 count | Reach 3 side channel count | Reach 4 upstream side channel count | Reach 4 downstream side channel count |
|---|---|---|---|---|---|---|---|
| organic | 0 | 0 | 0 | 0 | 0 | 0 | 1 |
| sand | 3 | 6 | 2 | 6 | 0 | 23 | 0 |
| 4 | 1 | 0 | 0 | 0 | 0 | 0 | 0 |
| 5.7 | 1 | 0 | 0 | 0 | 0 | 0 | 0 |
| 8 | 0 | 1 | 0 | 0 | 0 | 4 | 0 |
| 11.3 | 4 | 2 | 3 | 0 | 0 | 9 | 0 |
| 16 | 7 | 1 | 4 | 7 | 0 | 21 | 3 |
| 22.5 | 9 | 9 | 12 | 7 | 6 | 19 | 2 |
| 32 | 8 | 14 | 22 | 8 | 7 | 12 | 5 |
| 45 | 19 | 11 | 19 | 18 | 17 | 3 | 21 |
| 60 | 16 | 22 | 16 | 15 | 26 | 4 | 16 |
| 90 | 17 | 11 | 8 | 15 | 24 | 0 | 12 |
| 128 | 9 | 12 | 8 | 16 | 8 | 1 | 18 |
| 180 | 4 | 3 | 2 | 6 | 7 | 0 | 12 |
| 256 | 1 | 6 | 2 | 1 | 4 | 3 | 6 |
| 362 | 1 | 0 | 1 | 0 | 0 | 1 | 0 |
| boulder | 0 | 2 | 1 | 1 | 1 | 0 | 4 |

**Table A2 - Summary data for grain size distributions**

| | Reach 1 | Reach 2 | Reach 3 | Reach 4 | Reach 3 side channel | Reach 4 upstream side channel | Reach 4 downstream side channel |
|---|---|---|---|---|---|---|---|
| d16 (mm) | 16 | 22.5 | 22.5 | 22.5 | 45 | 1 | 15 |
| d50 (mm) | 45 | 60 | 45 | 60 | 60 | 16 | 90 |
| d84 (mm) | 90 | 128 | 90 | 128 | 128 | 32 | 180 |
| Gr | 2.41 | 2.4 | 2 | 2.4 | 1.73 | 9 | 2 |

**Table A3 - Reach 1 patchiness.** One clast was measured every meter walking upstream at river right, river left, and the center of the channel. All grain sizes are in mm.

| Station | River left | Center | River right |
|---|---|---|---|
| 0 | 32 | 32 | 60 |
| 1 | 32 | 45 | 45 |
| 2 | 22.5 | 128 | 32 |
| 3 | 32 | 60 | 16 |
| 4 | 45 | 22.5 | 32 |
| 5 | 45 | 45 | 22.5 |
| 6 | 60 | 22.5 | 22.5 |
| 7 | 22.5 | 60 | 90 |
| 8 | 8 | 60 | 45 |
| 9 | 128 | 32 | 45 |
| 10 | 32 | 60 | 32 |
| 11 | 45 | 256 | 32 |
| 12 | 11.3 | 90 | 128 |
| 13 | 16 | 180 | 90 |
| 14 | 45 | 128 | 5.7 |
| 15 | 60 | 60 | 60 |
| 16 | 22.5 | 45 | 180 |
| 17 | 1 | 16 | 128 |
| 18 | 1 | 45 | 256 |
| 19 | 60 | 60 | 180 |
| 20 | 60 | 60 | 128 |
| 21 | 90 | 90 | 128 |
| 22 | 256 | 60 | 60 |
| 23 | 128 | 60 | 90 |
| 24 | 128 | 90 | 22.5 |
| 25 | 90 | 128 | 90 |

**Table A4 - Reach 2 patchiness.** One clast was measured every meter walking upstream at river right, river left, and the center of the channel. All grain sizes are in mm.

| Station | River left | Center | River right | Station | River left | Center | River right |
|---|---|---|---|---|---|---|---|
| **0** | sand | 60 | 16 | **27** | 128 | 90 | 128 |
| **1** | sand | 45 | 180 | **28** | 128 | 256 | 60 |
| **2** | 22.5 | 90 | boulder | **29** | 90 | 256 | 60 |
| **3** | 90 | 45 | 22.5 | **30** | 90 | 60 | 32 |
| **4** | 180 | 60 | 90 | **31** | 45 | 128 | 22.5 |
| **5** | 45 | 60 | 60 | **32** | 45 | 60 | sand |
| **6** | sand | 45 | 90 | **33** | 90 | sand | 90 |
| **7** | 22.5 | 128 | 60 | **34** | sand | 90 | 90 |
| **8** | 60 | 60 | 60 | **35** | 128 | 32 | 256 |
| **9** | 256 | 128 | 32 | **36** | boulder | 60 | 45 |
| **10** | 16 | 90 | 128 | **37** | boulder | 256 | 362 |
| **11** | 90 | 90 | 60 | **38** | 90 | 180 | 128 |
| **12** | 32 | 16 | 180 | **39** | 128 | 90 | 32 |
| **13** | 60 | 60 | 90 | **40** | 128 | 90 | 60 |
| **14** | 256 | 22.5 | 60 | **41** | 45 | 180 | 45 |
| **15** | 32 | 60 | 22.5 | **42** | 60 | 180 | 32 |
| **16** | sand | 128 | sand | **43** | 45 | sand | 8 |
| **17** | sand | wood | wood | **44** | 128 | 60 | 90 |
| **18** | 90 | 362 | sand | **45** | 90 | sand | sand |
| **19** | 256 | 90 | sand | **46** | 256 | 90 | 8 |
| **20** | sand | 180 | sand | **47** | 45 | 28 | 128 |
| **21** | 22.5 | 128 | 16 | **48** | 90 | 90 | boulder |
| **22** | sand | 60 | 16 | **49** | 32 | 128 | 45 |
| **23** | 256 | 180 | 60 | **50** | 60 | 90 | 32 |
| **24** | 180 | 60 | boulder | **51** | 60 | 60 | 45 |
| **25** | 180 | 45 | 90 | **52** | 60 | 32 | 60 |
| **26** | 128 | 362 | 60 | | | | |

**Table A5 - Reach 3 patchiness.** One clast was measured every meter walking upstream at river right, river left, and the center of the channel. All grain sizes are in mm**.**

| Station | River left | Center | River right | Station | River left | Center | River right |
|---|---|---|---|---|---|---|---|
| **0** | 128 | 60 | 256 | **25** | org | 60 | organic |
| **1** | 45 | 60 | 128 | **26** | 90 | 90 | sand |
| **2** | 60 | 256 | 90 | **27** | 90 | sand | sand |
| **3** | 90 | 90 | 90 | **28** | 60 | sand | sand |
| **4** | 16 | 45 | 22.5 | **29** | 45 | sand | sand |
| **5** | 16 | 90 | boulder | **30** | 90 | sand | organic |
| **6** | sand | 45 | 60 | **31** | 90 | sand | 11.3 |
| **7** | sand | 45 | 90 | **32** | 60 | 90 | 45 |
| **8** | sand | 90 | 128 | **33** | 45 | 16 | 22.5 |
| **9** | 60 | 128 | 128 | **34** | 22.5 | 60 | 11.3 |
| **10** | 22.5 | 256 | 180 | **35** | 32 | sand | 16 |
| **11** | 45 | 90 | 45 | **36** | 45 | 60 | sand |
| **12** | 90 | 60 | sand | **37** | 180 | sand | organic |
| **13** | 90 | 180 | boulder | **38** | 90 | 128 | 32 |
| **14** | 128 | 128 | 90 | **39** | 22.5 | boulder | sand |
| **15** | 90 | 90 | 90 | **40** | 90 | 128 | sand |
| **16** | 60 | 90 | 22.5 | **41** | 180 | 90 | 45 |
| **17** | 90 | 128 | boulder | **42** | 45 | 22.5 | 45 |
| **18** | 32 | 32 | 60 | **43** | 32 | 45 | 32 |
| **19** | 16 | 90 | 60 | **44** | 362 | 90 | 32 |
| **20** | wood | wood | wood | **45** | 11.3 | 45 | 32 |
| **21** | organic | organic | organic | **46** | 16 | 90 | 32 |
| **22** | 45 | 90 | organic | **47** | 32 | 22.5 | 90 |
| **23** | 45 | 22.5 | organic | **48** | organic | 22.5 | 45 |
| **24** | 90 | 60 | organic | | | | |

**Table A6 - Reach 4 patchiness.** One clast was measured every meter walking upstream at river right, river left, and the center of the channel. All grain sizes are in mm**.**

| Station | River left | Center | River right | Station | River left | Center | River right |
|---|---|---|---|---|---|---|---|
| **0** | 256 | 60 | 60 | **50** | sand | 11.3 | 32 |
| **1** | 60 | 90 | 256 | **51** | sand | 11.3 | sand |
| **2** | 60 | 128 | 180 | **52** | sand | 22.5 | 11.3 |
| **3** | boulder | 128 | boulder | **53** | 60 | 22.5 | 45 |
| **4** | 60 | 180 | 180 | **54** | 22.5 | 32 | sand |
| **5** | 60 | 128 | boulder | **55** | 90 | 16 | sand |
| **6** | 90 | 60 | 128 | **56** | 60 | 11.3 | sand |
| **7** | 45 | 362 | 180 | **57** | 60 | 16 | sand |
| **8** | 32 | boulder | 128 | **58** | 45 | 32 | sand |
| **9** | 32 | 60 | 128 | **59** | 22.5 | 45 | 22.5 |
| **10** | sand | 32 | 90 | **60** | sand | 60 | 60 |
| **11** | sand | 180 | 22.5 | **61** | 60 | 60 | 45 |
| **12** | 22.5 | 60 | 60 | **62** | 45 | 60 | 22.5 |
| **13** | 45 | 60 | 90 | **63** | 32 | 16 | 60 |
| **14** | 45 | 90 | 60 | **64** | 32 | 60 | 11.3 |
| **15** | 45 | 128 | boulder | **65** | 22.5 | 45 | 90 |
| **16** | 90 | 90 | 45 | **66** | 45 | 22.5 | 32 |
| **17** | 45 | 128 | 90 | **67** | 256 | 60 | 45 |
| **18** | 60 | 180 | 60 | **68** | 60 | 32 | 90 |
| **19** | 60 | 90 | 128 | **69** | 128 | 45 | 16 |
| **20** | 256 | 45 | 60 | **70** | 60 | 60 | 60 |
| **21** | 16 | 90 | 90 | **71** | 90 | 90 | 22.5 |
| **22** | 60 | 60 | 32 | **72** | 90 | 90 | 60 |
| **23** | 128 | 90 | 90 | **73** | 90 | 60 | 60 |
| **24** | 180 | 60 | 60 | **74** | 90 | 90 | 60 |
| **25** | 128 | 90 | 45 | **75** | 90 | 90 | sand |
| **26** | 180 | 60 | boulder | **76** | 16 | 60 | 45 |
| **27** | 16 | 256 | 90 | **77** | 11.3 | 60 | 180 |
| **28** | 90 | 128 | 45 | **78** | sand | 45 | 180 |
| **29** | 45 | 180 | 22.5 | **79** | 45 | sand | 256 |
| **30** | 60 | 60 | 45 | **80** | 60 | 256 | sand |
| **31** | 32 | 90 | 60 | **81** | 90 | 90 | sand |
| **32** | 60 | 45 | 256 | **82** | 90 | 128 | 45 |
| **33** | 45 | 180 | 60 | **83** | 32 | 128 | 60 |
| **34** | 45 | 45 | 45 | **84** | 45 | 45 | 60 |
| **35** | 45 | 45 | 60 | **85** | 45 | 32 | 90 |
| **36** | 90 | 90 | 60 | **86** | 22.5 | 90 | 180 |
| **37** | 90 | 128 | 60 | **87** | 45 | 128 | 90 |
| **38** | 45 | 60 | 128 | **88** | 45 | 90 | 90 |
| **39** | 45 | 32 | 32 | **89** | 90 | 60 | 128 |
| **40** | sand | 32 | 180 | **90** | 45 | 60 | 22.5 |
| **41** | wood | wood | wood | **91** | 180 | 90 | 60 |
| **42** | wood | wood | wood | **92** | 128 | 22.5 | 90 |
| **43** | wood | wood | wood | **93** | 60 | 60 | 128 |
| **44** | sand | sand | sand | **94** | 32 | 90 | 180 |
| **45** | sand | sand | 90 | **95** | 45 | sand | 256 |
| **46** | sand | sand | 128 | **96** | 90 | 60 | 60 |
| **47** | sand | sand | 60 | **97** | 90 | 128 | 128 |
| **48** | sand | 90 | 90 | **98** | 60 | 60 | boulder |
| **49** | 11.3 | 60 | 60 | **99** | 128 | 22.5 | 128 |

**Table A7 - Reach 4 side channel patchiness.** One clast was measured every meter walking upstream at river right, river left, and the center of the channel. All grain sizes are in mm.

| Upstream Side Channel | | | | Downstream Side Channel | | | |
|---|---|---|---|---|---|---|---|
| **Station** | River left | Center | River right | Station | River left | Center | River right |
| **0** | boulder | organic | organic | **0** | 90 | 16 | 45 |
| **1** | organic | 256 | organic | **1** | 32 | 22.5 | 90 |
| **2** | organic | organic | 180 | **2** | 22.5 | 45 | 22.5 |
| **3** | organic | organic | organic | **3** | sand | 60 | boulder |
| **4** | boulder | sand | boulder | **4** | sand | 45 | 128 |
| **5** | sand | 180 | organic | **5** | 60 | 22.5 | 60 |
| **6** | 60 | sand | sand | **6** | 45 | 22.5 | 128 |
| **7** | 8 | 180 | sand | **7** | sand | 90 | 45 |
| **8** | boulder | 256 | 128 | **8** | boulder | 128 | 90 |
| **9** | boulder | 362 | 90 | **9** | 128 | 90 | 32 |
| **10** | organic | 128 | 128 | **10** | 180 | 45 | 45 |
| **11** | organic | organic | sand | **11** | 128 | sand | 90 |
| **12** | organic | sand | 11.2 | **12** | 180 | 45 | 128 |
| **13** | organic | 22.5 | 128 | **13** | 90 | 90 | 45 |
| **14** | 32 | 32 | 45 | **14** | 128 | 60 | 60 |
| **15** | 11.3 | sand | organic | **15** | 90 | 32 | 90 |
| **16** | organic | 11.3 | 8 | **16** | 60 | 60 | 128 |
| **17** | sand | 16 | 16 | **17** | 60 | 60 | 256 |
| **18** | sand | 22.5 | 16 | **18** | 128 | sand | 128 |
| **19** | 11.3 | 32 | 22.5 | **19** | 45 | boulder | 128 |
| **20** | sand | 22.5 | 32 | **20** | 90 | 128 | 180 |
| **21** | 90 | 45 | 22.5 | **21** | 60 | 128 | 128 |
| **22** | wood | wood | wood | **22** | boulder | 90 | 90 |
| | | | | **23** | boulder | boulder | 60 |
| | | | | **24** | 60 | boulder | 128 |
| | | | | **25** | 128 | boulder | 180 |
| | | | | **26** | 180 | 256 | 180 |
| | | | | **27** | 128 | 180 | boulder |
| | | | | **28** | boulder | 180 | 90 |
| | | | | **29** | 256 | 180 | 90 |
| | | | | **30** | 128 | 90 | 180 |
| | | | | **31** | 22.5 | 60 | 128 |
| | | | | **32** | 32 | 128 | 180 |
| | | | | **33** | 90 | 128 | 90 |
| | | | | **34** | 32 | 128 | 128 |
| | | | | **35** | 45 | wood | organic |
| | | | | **36** | organic | organic | organic |
| | | | | **37** | organic | organic | organic |
| | | | | **38** | organic | organic | organic |
| | | | | **39** | organic | organic | organic |
| | | | | **40** | organic | 362 | organic |
| | | | | **41** | organic | sand | 180 |
| | | | | **42** | wood | boulder | boulder |

## Appendix B - Geomorphic data

### Table B1 - Cross sectional data

| Cross Section | Valley width (m) | Bankfull width (m) | Bankfull depth (cm) |
|---|---|---|---|
| R1XS1 | 56 | 5.35 | 40 |
| R1XS2 | 56 | 5.1 | 40 |
| R1XS3 | 55.3 | 4.25 | 50 |
| R1XS4 | 55.2 | 4.9 | 55 |
| R1XS5 | 52.7 | 3.8 | 65 |
| R2XS0 | 50.8 | 5 | 55 |
| R2XS1 | 49.2 | 5.2 | 55 |
| R2XS2 | 50 | 5.7 | 65 |
| R2XS3 | 47.1 | 5.3 | 50 |
| R2XS4 | 50 | 7 | 60 |
| R3XS1 | 16.4 | 6.5 | 35 |
| R3XS2 | 23.5 | 8.5 | 75 |
| R3XS3 | 32 | 14.4 | 55 |
| R3XS4 | 32.4 | 16 | 60 |
| R3XS5 | 30.6 | 7.5 | 40 |
| R4XS1 | 26.5 | 4.4 | 45 |
| R4XS2 | 21.1 | 8.9 | 70 |
| R4XS3 | 24.6 | 18.1 | 85 |
| R4XS4 | 20.3 | 8.4 | 55 |
| R4XS5 | 24.3 | 4.8 | 45 |

### Table B2 - Reach 1 longitudinal profile of the thalweg

| Horizontal distance (m) | Relative elevation (m) |
|---|---|
| **1.1** | 0 |
| **3.5** | 0.12 |
| **5.8** | -0.04 |
| **8.3** | 0.08 |
| **11.6** | 0.11 |
| **15.2** | 0 |
| **18.2** | 0.01 |
| **19.4** | 0.21 |
| **20.8** | 0.29 |
| **22** | 0.45 |

**Table B3 - Reach 2 longitudinal profile of the thalweg**

| Horizontal distance (m) | Relative elevation (m) |
|---|---|
| 0 | 0 |
| 2 | 0.01 |
| 4.5 | 0.05 |
| 6.8 | 0.02 |
| 9.1 | 0.05 |
| 10.7 | 0.18 |
| 12.2 | 0.2 |
| 12.4[1] | 0.8[1] |
| 13.3 | 0.29 |
| 14.1 | 0.2 |
| 16.2 | 0.17 |
| 18 | 0.24 |
| 20.8 | 0.32 |
| 22.3 | 0.44 |
| 24 | 0.63 |
| 26 | 0.61 |
| 28 | 0.57 |
| 30.2 | 0.62 |
| 32.1 | 0.77 |
| 34 | 0.89 |
| 35.6 | 0.94 |
| 37 | 0.92 |
| 38.2 | 0.82 |
| 40.3 | 0.81 |
| 42.3 | 0.84 |
| 44.4 | 1 |
| 45.8 | 1.1 |
| 47 | 1.05 |

[1] Measurement taken on top of key jam. Value was not used in calculation of $\sigma_z$.

**Table B4 - Reach 3 longitudinal profile of the thalweg**

| Horizontal distance (m) | Relative Elevation (m) |
|---|---|
| 0 | 0 |
| 2.3 | 0.02 |
| 3.5 | 0.02 |
| 5.7 | 0.08 |
| 7.4 | 0.08 |
| 8.6 | 0.29 |
| 11 | 0.37 |
| 12.5 | 0.53 |
| 13.8 | 0.44 |
| 14.4[1] | 1.78[1] |
| 16.1 | 0.83 |
| 18.6 | 0.93 |
| 20.4 | 1.09 |
| 23.2 | 1.03 |
| 24.5 | 0.94 |
| 26.8 | 1.03 |
| 28.9 | 1 |
| 31 | 0.97 |
| 32.5 | 0.86 |
| 33.4 | 0.85 |
| 35 | 0.86 |
| 37.6 | 0.96 |
| 38.8 | 1.14 |

[1] Measurement taken on top of key jam. Value was not used in calculation of $\sigma_z$.

**Table B5 - Reach 4 longitudinal profile of the thalweg**

| Horizontal distance (m) | Relative elevation (m) | Horizontal distance (m) | Relative elevation (m) |
|---|---|---|---|
| 0 | 0 | 65.8 | 2.18 |
| 1.4 | -0.01 | 67.8 | 2.38 |
| 2.8 | 0.12 | 69.8 | 2.41 |
| 4 | 0.11 | 71.9 | 2.48 |
| 5.5 | 0.21 | 73.8 | 2.44 |
| 6.9 | 0.16 | 75.9 | 2.49 |
| 8.6 | 0.26 | 78 | 2.46 |
| 10.5 | 0.33 | 79.8 | 2.63 |
| 11.3 | 0.5 | 81.3 | 2.76 |
| 13 | 0.55 | 82.3 | 2.75 |
| 15 | 0.42 | 83.7 | 2.87 |
| 17.5 | 0.31 | 85.3 | 2.98 |
| 19.9 | 0.64 | 87.1 | 2.97 |
| 22.2 | 0.72 | 88.8 | 3.07 |
| 24.3 | 0.85 | 90.8 | 3.33 |
| 26.3 | 0.99 | 92.9 | 3.63 |
| 28.1 | 1.01 | 94.8 | 3.72 |
| 30 | 0.86 | 96.7 | 3.76 |
| 32 | 0.99 | 98.9 | 3.71 |
| 34.2 | 1.14 | 100.9 | 3.8 |
| 36 | 1.25 | 102.8 | 3.65 |
| 38 | 1.4 | 104.1 | 3.82 |
| 40.3 | 1.6 | 106 | 3.84 |
| 42.5 | 1.24 | 107.9 | 3.8 |
| 44.1 | 1.74 | 109.3 | 3.6 |
| 46.4 | 1.58 | 111.2 | 3.76 |
| 46.8[1] | 2.63[1] | 113.2 | 3.8 |
| 48.7 | 1.95 | 114.8 | 3.92 |
| 50.7 | 1.69 | 116.6 | 3.91 |
| 52.2 | 1.79 | 117.9 | 3.87 |
| 54.3 | 1.93 | 119.8 | 4.01 |
| 56.8 | 2.13 | 120.2 | 4.11 |
| 59.2 | 2.15 | 121.2 | 3.91 |
| 61.5 | 2.18 | 122.2 | 3.96 |
| 64.5 | 2.17 | 124.6 | 4.24 |

[1] Measurement taken on top of key jam. Value was not used in calculation of $\sigma_z$.

**Table B6 - Reach 4 upstream side channel longitudinal profile of the thalweg**

| Horizontal distance (m) | Relative elevation (m) |
|---|---|
| 0 | 0 |
| 2.2 | 0.11 |
| 4 | 0 |
| 5.2 | 0.01 |
| 6 | 0.24 |
| 7.9 | 0.36 |
| 9.8 | 0.36 |
| 11 | 0.45 |
| 13 | 0.55 |
| 15.4 | 0.64 |
| 17 | 0.66 |
| 19 | 0.7 |
| 21 | 0.68 |
| 21.2[1] | 1.26[1] |
| 21.5 | 0.61 |

[1] Measurement taken on top of key jam

**Table B7 - Reach 4 downstream side channel longitudinal profile of the thalweg**

| Horizontal distance (m) | Relative elevation (m) |
|---|---|
| 0 | 0 |
| 2 | -0.05 |
| 4 | 0.04 |
| 5 | 0.24 |
| 7 | 0.44 |
| 9 | 0.23 |
| 10.4 | 0.2 |
| 12.2 | 0.1 |
| 13.5 | 0.39 |
| 15.5 | 0.55 |
| 17.7 | 0.55 |
| 19.7 | 0.7 |
| 21.5 | 0.83 |
| 23.4 | 0.9 |
| 25.6 | 0.99 |
| 27.2 | 1.05 |
| 25.8 | 0.89 |
| 29.2 | 1.34 |
| 31.4 | 1.43 |
| 33.3 | 1.57 |
| 34.7 | 1.66 |
| 36.7 | 1.85 |
| 38.5 | 2.18 |
| 40.3 | 2.1 |
| 41.7 | 1.97 |
| 43.8 | 2.04 |
| 45.2 | 1.96 |
| 45.4[1] | 2.79[1] |

[1] Measurement taken on top of key jam

## Appendix C - Wood Data

### Table C1 - LW survey

| Piece ID | Reach | Length (cm) | Diameter (cm) | Volume (m^3) | Stab. | Decay | Orien. | Root Wad | Latitude | Longitude |
|---|---|---|---|---|---|---|---|---|---|---|
| LW1 | N/A | 320 | 11 | 0.030 | UN | D2 | PA | YES | 40.62006 | -105.53853 |
| LW2 | N/A | 140 | 13 | 0.019 | P | D2 | PA | NO | 40.62012 | -105.53851 |
| LW3 | N/A | 190 | 12 | 0.021 | P | D2 | PA | YES | 40.62013 | -105.53862 |
| LW4 | N/A | 280 | 18 | 0.071 | B | D4 | PE | NO | 40.6201 | -105.53867 |
| LW5 | N/A | 120 | 21 | 0.042 | UN | D4 | PE | NO | 40.62008 | -105.53876 |
| LW6 | N/A | 140 | 10 | 0.011 | LIVE | N/A | PA | NO | 40.62006 | -105.53878 |
| LW7 | N/A | 200 | 13 | 0.027 | RR | D3 | OB | NO | 40.62006 | -105.53878 |
| LW8 | N/A | 550 | 24 | 0.249 | UN | D4 | PA | NO | 40.6199 | -105.53904 |
| LW9 | N/A | 310 | 16 | 0.062 | B | D2 | PA | NO | 40.6199 | -105.53904 |
| LW10 | N/A | 660 | 15 | 0.117 | UN | D2 | PA | YES | 40.6198 | -105.53909 |
| LW11[3] | N/A | 480 | 18 | 0.122 | RR-B | D3 | PE | YES | 40.61975 | -105.5391 |
| LW12[3] | N/A | 420 | 22 | 0.160 | RR-B | D3 | PE | NO | 40.61975 | -105.5391 |
| LW13 | N/A | 160 | 65 | 0.531 | RL-B | D4 | PE | YES | 40.61962 | -105.5397 |
| LW14 | N/A | 670 | 18 | 0.170 | RL | D3 | PA | YES | 40.61959 | -105.53987 |
| LW15 | N/A | 170 | 13 | 0.023 | RR | D3 | OB | NO | 40.61959 | -105.53987 |
| LW16 | N/A | 170 | 12 | 0.019 | P | D2 | PA | NO | 40.61942 | -105.54015 |
| LW17 | N/A | 200 | 12 | 0.023 | RR | D3 | PE | NO | 40.61942 | -105.54015 |
| LW18 | N/A | 340 | 82 | 1.796 | B | D4 | OB | YES | 40.61939 | -105.54031 |
| LW19 | 2 | 250 | 12 | 0.028 | UN | D3 | OB | NO | 40.61919 | -105.54052 |
| LW20 | N/A | 330 | 38 | 0.374 | RR | D4 | PE | YES | 40.61889 | -105.54059 |
| LW21 | N/A | 350 | 28 | 0.216 | RR | D4 | PE | NO | 40.61888 | -105.54066 |
| LW22 | N/A | 170 | 12 | 0.019 | UN | D3 | PA | NO | 40.61884 | -105.5408 |
| LW23 | N/A | 295 | 11 | 0.028 | B | D4 | PA | NO | 40.61884 | -105.5408 |
| LW24 | N/A | 320 | 14 | 0.049 | UN | D4 | PA | NO | 40.61854 | -105.541 |
| LW25 | N/A | 230 | 12 | 0.026 | P | D3 | PA | NO | 40.61844 | -105.54105 |
| LW26 | N/A | 280 | 17 | 0.064 | UN | D2 | OB | NO | 40.61841 | -105.54104 |
| LW27 | N/A | 480 | 25 | 0.236 | RR | D3 | OB | NO | 40.61841 | -105.54104 |
| LW28 | N/A | 470 | 17 | 0.107 | B | D4 | PA | NO | 40.61841 | -105.54104 |
| LW29 | N/A | 170 | 13 | 0.023 | RL | D1 | PA | YES | 40.61825 | -105.54105 |
| LW30 | N/A | 480 | 20 | 0.151 | UN | D4 | PA | NO | 40.61823 | -105.54109 |
| LW31 | N/A | 170 | 11 | 0.016 | UN | D3 | PA | NO | 40.61823 | -105.54109 |
| LW32 | N/A | 670 | 35 | 0.645 | UN | D4 | PA | NO | 40.61814 | -105.5411 |
| LW33 | N/A | 1040 | 35 | 1.001 | UN | D4 | PA | NO | 40.61808 | -105.5411 |
| LW34 | N/A | 125 | 47 | 0.217 | B | D4 | PA | NO | 40.61797 | -105.54119 |
| LW35 | N/A | 770 | 29 | 0.509 | BR | D4 | OB | NO | 40.61789 | -105.54147 |
| LW36 | N/A | 400 | 21 | 0.139 | B | D4 | PE | NO | 40.61784 | -105.54151 |
| LW37 | N/A | 550 | 21 | 0.190 | B | D4 | PA | NO | 40.61755 | -105.54174 |
| LW38 | N/A | 245 | 12 | 0.028 | B | D4 | OB | NO | 40.61755 | -105.54174 |

| Piece ID | Reach | Length (cm) | Diameter (cm) | Volume (m^3) | Stab.[1] | Decay | Orien.[2] | Root Wad | Latitude | Longitude |
|---|---|---|---|---|---|---|---|---|---|---|
| LW39 | N/A | 230 | 12 | 0.026 | LIVE | N/A | PE | NO | 40.61755 | -105.54714 |
| LW40 | N/A | 300 | 12 | 0.034 | P | D3 | PA | NO | 40.61748 | -105.54177 |
| LW41[4] | N/A | 550 | 29 | 0.363 | B | D4 | PE | NO | 40.61738 | -105.54192 |
| LW42 | N/A | 260 | 12 | 0.029 | P | D4 | PA | NO | 40.61687 | -105.54216 |
| LW43 | N/A | 410 | 11 | 0.039 | UN | D3 | PA | NO | 40.61681 | -105.54221 |
| LW44 | N/A | 230 | 12 | 0.026 | B | D4 | PA | NO | 40.61681 | -105.54221 |
| LW45 | N/A | 270 | 32 | 0.217 | B | D4 | PA | NO | 40.61658 | -105.45234 |
| LW46 | N/A | 300 | 18 | 0.076 | B | D4 | PA | NO | 40.6164 | -105.54276 |
| LW47 | N/A | 190 | 14 | 0.029 | RR | D3 | OB | NO | 40.61628 | -105.54297 |
| LW48 | 3 | 865 | 19 | 0.245 | B | D1 | PA | NO | 40.61617 | -105.54314 |
| LW49 | 3 | 110 | 14 | 0.017 | B | D4 | OB | NO | 40.61617 | -105.54318 |
| LW50 | 3 | 120 | 10 | 0.009 | B | D4 | OB | NO | 40.61617 | -105.54318 |
| LW51 | 3 | 130 | 11 | 0.012 | RR | D3 | PE | NO | 40.61627 | -105.54324 |
| LW52 | 3 | 130 | 22 | 0.049 | UN | D4 | OB | NO | 40.61627 | -105.54324 |
| LW53 | 3 | 450 | 16 | 0.090 | RL | D4 | OB | NO | 40.61627 | -105.54324 |
| LW54 | 3 | 250 | 18 | 0.064 | B | D4 | PA | NO | 40.61628 | -105.54328 |
| LW55 | 3 | 330 | 23 | 0.137 | LIVE | N/A | PE | NO | 40.61628 | -105.54328 |
| LW56 | 6 | 120 | 20 | 0.038 | UN | D4 | PA | NO | 40.61628 | -105.54328 |
| LW57 | N/A | 580 | 15 | 0.102 | UN | D1 | OB | NO | 40.61629 | -105.54338 |
| LW58 | N/A | 110 | 17 | 0.025 | RR | D4 | PE | NO | 40.61629 | -105.54371 |
| LW59 | N/A | 100 | 20 | 0.031 | RR | D4 | OBL | NO | 40.61629 | -105.54371 |
| LW60 | N/A | 320 | 18 | 0.081 | B | D4 | PA | NO | 40.61626 | -105.54399 |
| LW61 | N/A | 370 | 21 | 0.128 | BR | D4 | PE | NO | 40.61629 | -105.54395 |
| LW62 | N/A | 190 | 18 | 0.048 | UN | D4 | OB | NO | 40.61633 | -105.54414 |
| LW63 | 4 | 280 | 12 | 0.032 | RL | D4 | PA | NO | 40.61649 | -105.54469 |
| LW64 | 4 | 110 | 18 | 0.028 | RL | D2 | OB | YES | 40.61652 | -105.54478 |
| LW65 | 4 | 170 | 40 | 0.214 | UN | D4 | PA | NO | 40.61654 | -105.54485 |
| LW66 | 4 | 125 | 44 | 0.190 | RL | D4 | OB | NO | 40.61656 | -105.54488 |
| LW67 | 4 | 330 | 14 | 0.051 | UN | D4 | PA | NO | 40.61657 | -105.5449 |
| LW68 | 4 | 250 | 12 | 0.028 | RR | D4 | OB | NO | 40.61657 | -105.5449 |
| LW69 | 4 | 230 | 15 | 0.041 | RR | D4 | OB | NO | 40.61659 | -105.54496 |
| LW70 | 4 | 240 | 23 | 0.100 | RR | D3 | PE | YES | 40.61671 | -105.54509 |
| LW71 | 4 | 440 | 12 | 0.050 | BR | D4 | PE | NO | 40.61691 | -105.5455 |
| LW72 | 4 | 360 | 22 | 0.137 | B | D4 | PE | YES | 40.61696 | -105.54557 |
| LW73 | 4 | 330 | 18 | 0.084 | RR | D4 | OB | NO | 40.61696 | -105.54557 |
| LW74 | 4 | 100 | 16 | 0.020 | RR | D4 | PE | NO | 40.61696 | -105.54557 |
| LW75 | 4 | 140 | 13 | 0.019 | B | D4 | PA | NO | 40.61653 | -105.54462 |
| LW76 | 4 | 130 | 27 | 0.074 | UN | D4 | PA | NO | 40.61657 | -105.54465 |
| LW77 | 4 | 110 | 24 | 0.050 | UN | D4 | PA | NO | 40.61657 | -105.54465 |
| LW78 | 4 | 310 | 15 | 0.055 | UN | D4 | PA | NO | 40.61666 | -105.54471 |
| LW79 | 4 | 100 | 33 | 0.086 | RL | D4 | OB | NO | 40.61666 | -105.54475 |

| Piece ID | Reach | Length (cm) | Diameter (cm) | Volume (m^3) | Stab. | Decay | Orien. | Root Wad | Latitude | Longitude |
|---|---|---|---|---|---|---|---|---|---|---|
| LW80 | 4 | 100 | 27 | 0.057 | RR | D4 | OB | NO | 40.61666 | -105.54475 |
| LW81 | 4 | 300 | 22 | 0.114 | P | D4 | OB | NO | 40.61677 | -105.54499 |
| LW82 | 4 | 220 | 12 | 0.025 | B | D3 | OB | NO | 40.61677 | -105.54499 |
| LW83 | 4 | 340 | 15 | 0.060 | RL | D4 | PA | NO | 40.61681 | -105.54511 |

[1] Stability. LW can be characterized as live, unattached (UN), bridge (BR), ramp left/right (RL/R), pinned (P), or buried (B). Pieces can be both buried and another characteristic i.e. RR-B

[2] Orientation. LW is characterized as either parallel (PA), perpendicular (PE), or oblique (OB)

[3] LW 11/12 have a plunge pool with a volume of 1.84 $m^3$

[4] LW 41 has a plunge pool with a volume of 5.71 $m^3$

**Table C2 - Jam survey. All jams are backwater pools unless noted otherwise**

| Jam ID | Reach | Span.[1] | RL (cm) | RW (cm) | RH (cm) | p[2] (%) | TV[3] ($m^3$) | PV[4] ($m^3$) | FV[5] ($m^3$) | Latitude | Longitude |
|---|---|---|---|---|---|---|---|---|---|---|---|
| J1 | N/A | P | 410 | 140 | 80 | 45 | 3.46 | 2.98 | --- | 40.6201 | -105.53881 |
| J2 | N/A | P | 190 | 130 | 40 | 70 | 1.04 | --- | --- | 40.62009 | -105.53899 |
| J3 | N/A | P | 380 | 190 | 90 | 75 | 2.42 | 3.5 | --- | 40.6199 | -105.53904 |
| J4 | 2 | F | 350 | 80 | 40 | 60 | 0.62 | 2.39 | 0.61 | 40.6192 | -105.5405 |
| J5 | 2 | P | 150 | 110 | 90 | 60 | 2.59 | --- | --- | 40.61896 | -105.54054 |
| J6 | N/A | P | 670 | 60 | 65 | 20 | 2.89 | --- | 4.75 | 40.61886 | -105.54062 |
| J7 | N/A | P | 490 | 180 | 85 | 35 | 5.42 | --- | --- | 40.61882 | -105.54074 |
| J8 | N/A | C | N/A | N/A | N/A | N/A | 0.31 | --- | 1.16 | 40.61887 | -105.5407 |
| J9 | N/A | F | 310 | 1430 | 45 | 45 | 21 | 2.7 | 5.51 | 40.61846 | -105.54078 |
| J10 | N/A | P | 190 | 55 | 20 | 20 | 0.48 | --- | --- | 40.61854 | -105.541 |
| J11 | N/A | P | 160 | 45 | 40 | 40 | 0.17 | --- | --- | 40.61823 | -105.54109 |
| J12 | N/A | P | 100 | 50 | 60 | 60 | 0.08 | --- | --- | 40.61789 | -105.5413 |
| J13 | N/A | P | 130 | 230 | 25 | 25 | 2.12 | 2.28 | --- | 40.61784 | -105.54146 |
| J14 | N/A | P | 470 | 65 | 70 | 70 | 0.61 | --- | --- | 40.61784 | -105.54151 |
| J15 | N/A | P | 240 | 45 | 30 | 30 | 0.41 | --- | --- | 40.61699 | -105.54209 |
| J16 | N/A | P | 200 | 40 | 40 | 40 | 0.23 | --- | --- | 40.61665 | -105.54225 |
| J17 | N/A | P | 200 | 40 | 45 | 50 | 0.44 | --- | --- | 40.61652 | -105.54248 |
| J18 | 3 | F | 810 | 165 | 100 | 40 | 9.71 | 30.56[6] | 9.62 | 40.61614 | -105.54307 |
| J19 | 3 | P | 80 | 40 | 25 | 60 | 0.07 | --- | --- | 40.6162 | -105.54314 |
| J20 | N/A | P | 140 | 50 | 35 | 35 | 0.63 | --- | --- | 40.61629 | -105.54371 |
| J21 | N/A | P | 230 | 110 | 70 | 80 | 0.19 | --- | --- | 40.61632 | -105.54409 |
| J22 | N/A | P | 500 | 80 | 60 | 60 | 1.02 | --- | --- | 40.61646 | -105.54446 |
| J23 | 4 | P | 140 | 30 | 35 | 70 | 0.08 | --- | --- | 40.61649 | -105.54469 |
| J24 | 4 | P | 30 | 60 | 25 | 60 | 0.04 | --- | --- | 40.61659 | -105.54496 |
| J25 | 4 | P | 60 | 35 | 35 | 40 | 0.08 | --- | --- | 40.61659 | -105.54496 |
| J26 | 4 | F | 480 | 160 | 90 | 40 | 4.97 | 7.31 | 2.04 | 40.61664 | -105.54501 |
| J27 | 4 | P | 120 | 30 | 30 | 80 | 0.03 | --- | 0.06 | 40.61668 | -105.54516 |
| J28 | 4 | P | 65 | 90 | 65 | 75 | 0.02 | --- | --- | 40.61674 | -105.54525 |
| J29 | 4 | P | N/A | N/A | N/A | N/A | 0.02 | --- | --- | 40.61676 | -105.54528 |
| J30 | 4 | F | 380 | 70 | 40 | 45 | 0.73 | --- | --- | 40.61678 | -105.54534 |
| J31 | 4 | P | 250 | 60 | 35 | 70 | 0.21 | --- | --- | 40.61684 | -105.54547 |
| J32 | 4 | P | 75 | 30 | 30 | 40 | 0.08 | --- | --- | 40.6169 | -105.5455 |
| J33 | 4 | P | 130 | 20 | 20 | 10 | 0.06 | --- | 0.045 | 40.61667 | -105.54491 |
| J34 | 4 | F | 360 | 260 | 60 | 60 | 4.28 | --- | 0.375 | 40.61671 | -105.54499 |
| J35 | 4 | P | 60 | 60 | 40 | 30 | 0.18 | --- | --- | 40.61667 | -105.54491 |
| J36 | 4 | P | 45 | 45 | 35 | 220 | 0.23 | 1.748 | --- | 40.61683 | -105.54522 |

[1] Spanning. Jams are characterized as partially spanning (P) or fully spanning (F)

[2] Porosity

[3] Total Volume of each jam

[4] Pool volume at each jam

[5] Volume of accumulated fine material at each jam

[6] J18 also has a plunge pool with a volume of 1.93 $m^3$